The role of human cord blood endothelial colony forming cell-derived extracellular vesicles in acute kidney injury (AKI)

Randa Haneef

Thesis submitted to the Faculty of Graduate and Postdoctoral Studies in partial fulfilment of the requirements for the degree of Master of Science, Cellular and Molecular Medicine

Department of Cellular and Molecular Medicine
Faculty of Medicine
University of Ottawa

Abstract:

Acute kidney injury (AKI) is a sudden reduction in renal function, associated with a high mortality rate. The main cause of AKI is ischemia reperfusion injury. We previously found that administration of endothelial colony forming cells (ECFCs) or their derived exosomes protects ischemic renal cells against ischemia via paracrine action. Moreover, ECFC-derived exosomes are highly enriched with miRNA-486-5p, which protects against ischemia. Unexpectedly, ECFC infusion into mice with AKI attenuates renal endothelial cell proliferation. Therefore, we examined the role of ECFC-derived exosomes and microparticles (MPs) on endothelial cell angiogenic properties (proliferation and migration) *in vitro*, the pathways by which exosomes get internalized into endothelial cells, and the effects of miRNA-486-5p on endothelial cell migration. **Results:** ECFC-derived exosomes and MPs enhance endothelial cell proliferation in hypoxia and normoxia, and improve cellular migration. Finally, miRNA-486-5p plays a role in inducing HUVEC migration in normoxia. **Conclusion:** These findings indicate that ECFC-derived exosomes and MPs protect endothelial cells against ischemia by activating cellular migration, and that miRNA-486-5p plays a role in endothelial cell recovery after ischemia.

Table of contents

Acknowledgements

I accomplished this work with the support of many individuals, to who I would like to express my deepest appreciation. I would first like to thank my thesis advisor Dr. Kevin Burns. Dr. Burns was always there whenever I encountered challenges or had questions about my research. He provides me with continuous support. My appreciation is next extended to my committee members Dr. Chris Kennedy and Dr. Dylan Burger, for providing suggestions and guidance during committee meetings. Next is a heartfelt thanks to my lab members Dr. Jose Viñas, and KRC members for sharing their ideas, encouragement and support throughout my project, and to my friends Rajaa, Saeedah and Haya for being always around supporting me. Finally, I must express my profound gratitude to my family, especially my grandparents, my mother and uncle Abdulaziz Ibrahim for providing me with their support and continuous encouragement throughout my years of study. I would like to dedicate this thesis to the memory of my father, Abdulqayoom Haneef, whose words and advice kept me moving forward, and to my lovely siblings Donya, Shahad, and Badr.

Sources of funding

This research project is financially supported by the Canadian Institutes of Health Research (CIHR), and a full academic scholarship from the government of Saudi Arabia

List of figures

List of abbreviations

AKI	Acute kidney injury
Akt	Protein kinase B
Ab	Antibody
BMSC	Bone marrow-derived mesenchymal stem cell
BrdU	5-bromo-2'-deoxyuridine
BSA	Bovine serum albumin
BUN	Blood urea nitrogen
CDC	Cell division control protein
CFU-EC	Colony forming unit endothelial cells
CKD	Chronic kidney disease
CM	Conditioned media
CPZ	Chlorpromazine
CTL	Control
DC	Detergent compatible
DMSO	Dimethyl sulfoxide
DW	Distilled water
EA.hy926	Permanent human cell line
EBM-2	Endothelial Basal Media-2
ECFC	Endothelial colony forming cells

EDTA	Ethylenediaminetetraacetic acid
EdU	5-ethyle-2`-deoxyuridine
EIPA	Ethyl-isopropylamiloride
ELISA	Enzyme-linked Immunosorbent assay
eNOS	Endothelial nitric oxide synthase
EPC	Endothelial Progenitor Cells
ESCRT	Endosomal sorting complexes required for transport
EV	Extracellular vesicles
EX	Exosomes
FBS	Fetal Bovine Serum
G1-G2	Gap 1- Gap2
GAPDH	Glyceraldehyde 3-phosphate dehydrogenase
GFR	Glomerular filtration rate
HEK 293	Human embryonic kidney cells 293
hPMEC	Human Pulmonary Microvascular Endothelial Cells
H/R	Hypoxia/reoxygenation
HUVEC	Human umbilical vein endothelial cells
ICAM-1	Intercellular adhesion molecule-1
iMSC	Induced mesenchymal stem cells
ILVs	Intraluminal vesicles

IRI	Ischemia reperfusion injury
LSGS	Low Serum Growth Supplement
LY294002	Morpholine-containing chemical compound
M	Mitosis
mRNA	Messenger RNA
miRNA	Micro RNA
MSC	Mesenchymal stem cells
MP	Microparticles
MVs	Microvesicles
MVB	Multi vesicular bodies
NOD-SCID	Non obese diabetic/severe combined immunodeficient
ONFH	Osteonecrosis of the Femoral Head
PBS	Phosphate buffered saline
PCNA	Proliferating cell nuclear antigen
PCR	Polymerase chain reaction
Pre-miR	Precursor micro RNA
PTC	Proximal tubule cell
PTEN	Phosphatase and tensin homolog
REC	Renal endothelial cells
RIPA	Radioimmunoprecipitation assay buffer

ROS	Reactive oxygen species
SASP	Senescence-Associated Secretory Phenotype
SDS	Sodium dodecyl sulfate
TBM	Tetramethyl-benzidine
TBS-T	Tris-buffered saline containing 0.1% Tween 20
TGF-beta	Transforming growth factor beta
TNF-alpha	Tumor necrosis factor alpha
TSG101	Tumor susceptibility gene
VEGF	Vascular endothelial growth factor

Chapter 1: Introduction

1. 1. Acute Kidney Injury (AKI):

1. 1. 1. Definition and causes:

Acute kidney injury (AKI) is referred to as a sudden reduction in kidney function, ranging from a few hours to a few days (Bonventre and Yang, 2011). This is characterized by both structural damage (injury) and functional loss (impairment) (Makris and Spanou, 2016) with a high mortality rate (30% to 70% of AKI patients) (Bonventre and Yang, 2011), and rapid decrease in the glomerular filtration rate (GFR) which means reduction in glomerular hydrostatic pressure (Sharfuddin and Molitoris, 2011). Different factors can cause AKI, including sepsis, ischemia, and nephrotoxicity (Makris and Spanou, 2016), although renal ischemia/reperfusion injury (IRI) is the most common cause (Bonventre and Yang, 2011). IRI may occur from blood loss after cardiac surgery, or the use of vasoconstrictive drugs (Bonventre and Yang, 2011), which reduce the delivery of oxygen and nutrients to renal cells. This leads to inflammation and oxidative stress, which results in the development of AKI (Bonventre and Yang, 2011).

1. 1. 2. AKI pathophysiology and renal repair:

AKI pathogenesis involves a complex set of cellular interactions, beginning with disruption to the cytoskeletal integrity of tubular cells, and subsequent shedding of tubular cells into the lumen, resulting in tubular obstruction, leading to a reduction in GFR (Bagshaw et al., 2010). In addition, an acute reduction in renal blood flow occurs in AKI, and contributes to the loss of GFR (Basile and Yoder, 2014).

The consequences of ischemic insult begin a few minutes after blood flow is restored (reperfusion); however, within hours, renal blood flow is reduced subsequently (Basile and Yoder, 2014). Because of the reduction in renal blood flow following ischemia, the blood vessels that supply endothelial cells and small arteriolar cells with nutrients undergo vasoconstriction in response to high levels of vasoconstrictive agents, such as endothelin-1 after ischemia (Bonventre and Yang, 2011). Injury to endothelial cells is involved in a functional loss of the capillary barrier that separates the lumen of the blood vessel from the surrounding tissue (Sharfuddin and Molitoris, 2011). Damaged endothelial cells endure several consequences, such as disruption of the actin cytoskeleton, alteration of endothelial cell contact, and breakdown of the perivascular matrix

(Bonventre and Yang, 2011). Thus, microvascular permeability is increased during AKI, leading to a loss of fluid into the interstitium (Bonventre and Yang, 2011). Furthermore, damaged endothelial cells upregulate the expression of intercellular adhesion molecule-1 (ICAM-1), which induces leukocytes to activate endothelial-leukocyte adhesion and promote coagulation, which results in capillary obstruction (Bonventre and Yang, 2011).

It has been known that renal cells have a high capacity for regeneration after ischemia, which is dependent on the proliferation of surviving tubular cells (Bagshaw et al., 2010; Basile and Yoder, 2014; Li et al., 2012). Many studies suggest that the mechanism of renal recovery is associated with a return of renal blood flow to baseline levels within days, and that the histological structure recovers within weeks (Basile and Yoder, 2014). During recovery after AKI, surviving tubular cells undergo de-differentiation, followed by migration along the basement membrane, proliferation and, finally, differentiation to restore nephron function (Canaud and Bonventre, 2015). However, the ability to recover after injury may not occur, and AKI instead can leads to abnormal repair with persistent parenchymal inflammation, fibroblast proliferation and excessive deposition of extracellular matrix (Canaud and Bonventre, 2015). Moreover, DNA

damage in tubular cells caused by toxins or ischemia can lead to cell senescence. Furthermore, severe AKI can cause tubular cell cycle arrest at the G2/M phase with activation of the "senescence-associated secretory phenotype"(SASP) (Canaud and Bonventre, 2015). Cell senescence lead to secretion of pro-proliferative and profibrotic factors, which can then lead to chronic inflammation and development of chronic kidney disease (CKD) (Canaud and Bonventre, 2015). Therefore, in some cases, many AKI patients do not fully recover, and they develop CKD (Bagshaw et al., 2010; Basile and Yoder, 2014; Li et al., 2012).

It has been indicated that the reduction in proximal tubular cell (PTC) density (important for growth factors expression) after ischemia is consistent with the notion that renal capillaries have a limited intrinsic regenerative capacity, which could be caused by a lack of nutrient elements that support (e.g. Vascular endothelial growth factor (VEGF)) capillary regeneration after ischemia (Basile, 2014). The expression of VEGF on renal epithelial cells is a main source of nutritional vascular support, and losing VEGF activity may lead to impaired repair (Basile and Yoder, 2014). Also, it has been suggested that there is an increase in the inhibitory factors that attenuate endothelial cells stability, such as Transforming growth factor beta (TGF)-beta (Basile and Yoder, 2014). Moreover, some endothelial growth

inhibitors are released after ischemia, such as angiostatin (Basile and Yoder, 2014).

As a therapeutic approach, efforts to minimize ischemia and its consequences can limit AKI and prevent the development of CKD. Unfortunately, there is no specific treatment available to restore kidney function and enhance cellular proliferation. However, recent evidence suggests that endothelial progenitor cells (EPCs) have a high ability to improve kidney regeneration (Liang et al., 2015),

1. 2. Cell Therapy in AKI:

Endothelial progenitor cells (EPCs) are circulating, bone marrow-derived precursors that can induce regeneration processes in ischemic tissues (Cantaluppi et al., 2012). Furthermore, EPCs promote many activities, two of which are vasculogenesis, an embryonic mechanism to form new blood vessels from mature endothelial cells (ECs), and angiogenesis, a mechanism that generates new vessels from pre-existing ones (Napoli et al., 2011). In 1997, Asahara et al. first described in detail the classical isolation process and function of EPCs (Asahara et al., 1997; Hristov et al., 2003). The isolation was initiated by separating CD34-positive monocular blood cells from human peripheral blood by magnetic microbeads, followed by plating

on fibronectin-coated surfaces with specific growth factors (e.g., VEGF, bovine brain extract, and epidermal growth factor) (Asahara et al., 1997; Hristov et al., 2003). These cells then developed into cells that gained endothelial characteristics. In addition to CD34, early EPCs express stem cell marker molecules (CD133, c-Kit) and endothelial lineage markers (Flk-1, CD31, eNOS) (Asahara et al., 1997; Hristov et al., 2003; Patschan et al., 2011). EPCs are able to differentiate into two main populations (Patschan et al., 2011). The first population can be isolated from human and animal peripheral blood circulation (Patschan et al., 2011). In vitro, this population can be cultured on fibronectin- coated dishes and cells appear after 5-7 days, identified as "early out-growth" EPCs. "Early out-growth" EPCs can express stem cell markers (e.g. CD133, c-Kit), and endothelial lineage markers (e.g. CD31, eNOS) (Patschan et al., 2011). "Early out-growth" EPCs are similar to "colony forming unit endothelial cells" (CFU-ECs), and can be isolated and cultured from mononuclear blood cells from different origins (Patschan et al., 2011). CFU-ECs can be cultured on fibronectin within two days and the nonadherent cells replated on new petri dishes where they produce colonies (Patschan et al., 2011). The second EPC population can be isolated from mononuclear cells and cultured on dishes coated with collagen type 2 (Patschan et al., 2011). Cells appear in the culture after 2-3 weeks and are

identified as “late out-growth” EPCs, also known as endothelial colony forming cells (ECFCs), and they express endothelial cell markers only (Patschan et al., 2011).

Human cord blood-derived ECFCs represent our cell of interest because they display similar vasculogenic activity as do mature EPCs, and the quantity of ECFCs in umbilical cord blood is higher than in peripheral blood (Moubarik et al., 2011). The ability of these cells to demonstrate natural vasculogenic properties, incorporate into the systemic vasculature of the host animal, and remodel into arteries and veins *in vivo*, distinguishes ECFCs from all other population of EPCs (Yoder, 2012).

Yamamoto and Brodsky were the first to suggest a new therapeutic approach to treat ischemic AKI. This approach involved targeting postischemic renal endothelial dysfunction to optimize renal reperfusion (Brodsky et al., 2002; Patschan et al., 2011; Yamamoto et al., 2002). They injected male athymic nude ischemic rats via jugular vein with human umbilical vein endothelial cells (HUVECs) or embryonic kidney cells (HEK-293), which exhibit stable expression of human endothelial nitric oxide synthase (eNOS) (Brodsky et al., 2002). The infusion of HUVECs into the rat after the renal artery clamp (ischemia) prevented the elevation of

blood serum creatinine (renal functions marker), associated with a lower degree of renal injury (Brodsky et al., 2002). Moreover, the injection of the HEK cells that expressed human eNOS enhanced renal function in ischemia, compared to HEK cells that were devoid of eNOS (Brodsky et al., 2002). Several animal and human studies have demonstrated that different types of progenitor/stem cells can restore the function of ischemic organs stimulating vasculogenesis and angiogenesis in ischemic areas, or by inducing re-endothelialization of injured blood vessels (Grange et al., 2014a; Hristov et al., 2003). Grange et al. reported that injecting labeled CD133+ (cell surface marker for undifferentiated stem/progenitor cell) progenitor cells, derived from the human renal medulla and mesenchymal stem cells (MSC), into mice with glycerol-induced AKI, caused a reduction in plasma blood urea nitrogen (BUN) and creatinine concentration. In addition, CD133+ progenitor cell infusion into mice significantly increased epithelial cell proliferation, reduced apoptotic cells and tubular casts in an AKI model (Grange et al., 2014a). In addition, CD133+ progenitor/stem cells have been detected in kidneys with AKI, through optical imaging (Grange et al., 2014). Burger et al. found a different effect when they infused human umbilical cord-blood derived CD133+ cells into mice with AKI at reperfusion (Burger et al., 2012). They found, unexpectedly, that CD133+

aggravated I/R-induced renal injury in mice. This effect was associated with increased inflammation (i. e. high TNF-alpha), increase in tubular cell apoptosis, and no change in the tubular cell proliferation rate (Burger et al., 2012). In addition, CD133+ cells showed no sign of homing to kidneys after ischemia (Burger et al., 2012). In conclusion, cell therapy can protect renal cells against ischemia and ameliorate renal function, but this effect varies from cell to cell (i.e. cell-specific effect).

Burger et al. demonstrated the effects of human cord blood-derived ECFCs in a mouse model of I/R AKI. Human cord blood-derived ECFCs were injected (10^6cells/injection) into Non obese diabetic/severe combined immunodeficiency (NOD-SCID) mice with AKI, with significant improvement in plasma blood urea nitrogen (BUN) and creatinine at 24 and 72 hrs after reperfusion occurred, which was associated with preserved renal histology (Burger et al., 2015). Furthermore, our lab concluded that ECFCs decreased inflammation, characterized by a reduction of macrophage infiltration and reactive oxygen species (ROS) generation (Burger et al., 2015). Cellular proliferation was determined by staining for proliferating cell nuclear antigen (PCNA) (Burger et al., 2015). Following 72 hours, mice with ischemia/reperfusion (I/R) displayed a significant ($P < 0.001$ VS sham) increase in kidney PCNA staining, which was mostly of tubular cell origin

(eNOS negative staining) (Burger et al., 2015). In contrast, AKI mice treated with ECFCs had attenuated cell proliferation at both selected time points (24 and 72 hours). Kidney I/R caused a significant increase in endothelial cell proliferation at 72 hrs, as detected by co-staining for eNOS. Treatment with ECFCs markedly suppressed the I/R-induced increases in endothelial proliferation **(Figure 1)** (Burger et al., 2015)**.**

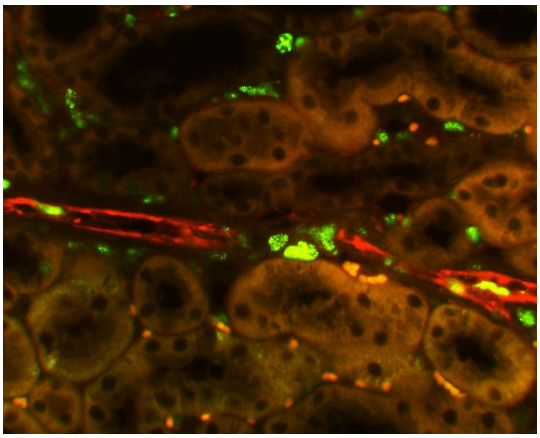

Figure 1: The effect of ECFCs on renal endothelial cell proliferation after I/R- induced AKI. Dr. Gutsol obtained this image. This experiment were done by Dr. Burger, and it showed the effect of human umbilical cord-blood–derived ECFC infusion into NOD-SCID mice at reperfusion in I/R-induced renal injury at 72 hours. Endothelial nitric oxide synthase (eNOS) (red) and PCNA (green)-positive cells in kidney sections following -I/R at 72 hrs.

On the one hand, progenitor/stem cell transplantation aims to target ischemic cells and improve tissue function (Baraniak and McDevitt, 2010). On the other hand, it has become clear that functional improvements may result from paracrine actions in host tissues rather than cell incorporation (Baraniak and McDevitt, 2010).

1. 3. Extracellular vesicles:

Extracellular vesicles (EVs) are released from different cell types into the extracellular environment (Burger et al., 2013; Colombo et al., 2014). They can be isolated from many biological fluids, such as blood and urine (Burger et al., 2013; Colombo et al., 2014). Depending on their size, they are identified as apoptotic bodies, microparticles, or exosomes (Burger et al., 2013; Colombo et al., 2014). Apoptotic bodies are large, ranging between 1-5 μm in diameter. They are formed as blebs during the last stage of apoptosis, from all cell types, and act in horizontal transfer of oncogenes and DNA (Burger et al., 2013; György et al., 2011).

Microparticles (MPs) (100 nm – 1 μm) result from blebbing directly from the plasma membrane, and can be isolated from cultured cell medium and body fluids (van Balkom et al., 2011; Burger et al., 2013). Human bone marrow mesenchymal stem cell (MSC)-derived MPs have been found to be

involved in the horizontal transfer of genetic material to activate proliferation and decrease apoptosis of tubular epithelial cells *in vitro* (Choi et al., 2014).

In contrast, exosomes are formed via fusion of multivesicular bodies (MVBs) into the plasma membrane, and range from 40 to 100 nm in diameter (van Balkom et al., 2011). They can be isolated from various types of cells, body fluids (van Balkom et al., 2011), and cell culture supernatant. In this project we have focused on exosomes. Exosomes contain proteins (e.g., TSG101), mRNAs, miRNAs (miRs), lipids (e.g., cholesterol), and other cytosolic contents (van Balkom et al., 2011). Although there are several mechanisms leading to formation of exosomes from the fusion of MVBs, the featured mechanism is called endosomal-sorting complexes required for transport (ESCRT) (Farooqi et al., 2017). ESCRT is a pathway that recognizes ubiquitylated proteins, and ESCRT has four subunits in a complex numbered ESCRT-0, ESCRT-1, ESCRT-2, and ESCRT-3 (Farooqi et al., 2017). These subunits contain proteins that are able to recognize ubiquitinated cargos. ESCRT-0 complex enrolls proteins for internalization. ESCRT-1 and -2 define the budding process to promote de-ubiquitination of cargo proteins prior to formation of intraluminal vesicles (ILVs), and form MVBs in the intracellular compartment (Farooqi et al., 2017). The ESCRT-3

complex maintains the final stage in exosome biogenesis, before the vesicles get secreted (Farooqi et al., 2017).

Many studies have reported the role of exosomes in intercellular communication with target cells (Yamamoto et al., 2002). These interactions may occur through exosome adhesion with the recipient cell surface to stimulate signaling pathways (Colombo et al., 2014). Exosomes may also fuse their contents either directly into the target cells, or incorporate the contents of recipient cells through endocytosis (Colombo et al., 2014).

1. 3. 1. Extracellular vesicles in AKI:

The Camussi group studied the effect of administrating a mix of microvesicles (MVs), which were obtained from peripheral blood-derived EPCs, in acute renal IRI rats *in vivo*. They also studied the mechanisms of MV protection from hypoxia-induced endothelial and epithelial kidney cell injury *in vitro* (Cantaluppi et al., 2012). Their results showed that MVs increase tubular proliferation and angiogenesis, which is associated with a remarkable decrease in cell apoptosis and leukocyte infiltration (Cantaluppi et al., 2012). In addition, they investigated the possibility of mesenchymal stem cell (MSC)-derived EVs as a potential therapeutic approach for AKI treatment, by visualizing the Vybrant Cell Tracers DiI labeled EVs in the

renal proximal tubular epithelial cells *in vitro*, and in dissected renal tissues, after 5 hrs and 24 hrs, using optical imaging *in vivo* (Grange et al., 2014). Results have shown that after AKI mice were injected with labeled EVs, MSC-derived EVs were detected in the kidneys after five hours and were maintained up to 24 hrs after injection. Confocal microscopy revealed that the labeled EVs were incorporated into proximal tubular epithelial cells after five hours of incubation *in vitro* (Grange et al., 2014b).

Another group labeled exosomes isolated from the melanoma cell line B16-BL6 with PKH26, and injected 5 μg of labeled exosomes via the tail vein into BALB/c mice (Takahashi et al., 2013). Animals were sacrificed at 10 minutes, 30 minutes, 60 minutes, and 240 minutes, and tissues from the liver, kidneys, spleen, and lung were collected for frozen section and microscopic examination (Takahashi et al., 2013). The results showed that after 30 and 240 minutes, the fluorescent labeling was detected in liver, spleen, and lung. Low fluorescence, however, was observed in kidney sections after four hours (Takahashi et al., 2013).

In 2012, The Camussi group demonstrated that the extracellular vesicles (EVs) derived from EPCs internalized into endothelial cells to transfer mRNAs and activate angiogenic pathways, and in 2015 they

suggested that miRNA in EVs derived from mesenchymal stromal cells have an important role in the regenerative potential of MSCs. Drosha knockdown in MSCs led to a global reduction in miRNA expression. This miRNA downregulation contributed to inhibition of the ability of MSCs and MSCs-derived EVs to promote AKI recovery (Cantaluppi et al., 2012; Collino et al., 2015).

In our lab, we investigated the role of ECFC-derived exosomes/MPs on endothelial cell apoptosis by examining terminal deoxynucleotidyl transferase-mediated dUTP nick-end labeling (TUNEL) staining and renal caspase-3 activity. HUVECs were subjected to hypoxia (94.5% N_2, 5% CO_2, and 0.5% O_2) in at 37 ^oC for 24 hours. Following hypoxia, cells were placed under normoxia conditions for reoxygenation for 24 hrs. Endothelial cells were treated with exosomes, and this reduced apoptosis, detected by Caspase-3 cleavage and activity (Burger et al., 2015). In addition, when H/R endothelial cells were treated with ECFC-conditioned media, this suppressed apoptosis and reduced the expression of ICAM-1 (Burger et al., 2015). On the other hand, treatment with MPs or ECFC-conditioned medium devoid of vesicles had no significant effect on both apoptosis and ICAM-1 expression in H/R endothelial cells (Burger et al., 2015).

1. 3. 2. EVs in endothelial cell proliferation

Blood vessels are essential for supplying nutrients and oxygen for tissue growth and repair (Wang et al., 2015). A process called angiogenesis is activated in response to ischemia. During angiogenesis, new capillaries are formed from pre-existing vessels, followed by cell proliferation and migration (Wang et al., 2015). In addition, growth factors induce the procession of the cell cycle. The cell cycle is divided into G1 (first gap), S (DNA synthesis), G2 (second gap), and M (mitosis)) (Berridge, 2014; Fukuhara et al., 2014).

Hu et al. examined the effect of induced pluripotent stem cell (MSC)-derived exosomes on HUVECs in a dose-dependent manner (iMSC-exosomes (0, 12.5, 25, 50, and 100 μg/mL) in *in vitro* (Hu et al., 2015*)*. They found that iMSC- derived exosomes enhance HUVEC proliferation (Hu et al., 2015).

Another study revealed that exosomes released from induced pluripotent mesenchymal stem cells (iPS-MSC-Exos) play a pivotal role in protecting ischemic connective tissues (Liu et al., 2017). In a model of osteonecrosis of the femoral head (ONFH), which is mainly caused by ischemia, this group examined the effect of iPS-MSC-Exos on HUVEC proliferation under low

serum growth supplement (LSGS), which contained iPS-MSC-Exos. Their findings showed a significant increase in HUVECs proliferation after iPS-MSC-Exos treatment (Liu et al., 2017).

1. 3. 3. EVs in endothelial cell migration

Endothelial cell migration is an important component of the angiogenesis process (Wang et al., 2015). Actin is a major cytoskeletal component of endothelial cells. The actin cytoskeleton is composed of filopodia, lamellipodia, and stress fibers, which are crucial in the regulation of endothelial cell migration (Lamalice et al., 2007). Filopodia are membrane projections that contain long, parallel actin filaments arranged into tight bundles. These filaments sense the motile stimulators (Lamalice et al., 2007). Filopodia formation is regulated by activation of cell division control (Cdc42) protein (Lamalice et al., 2007). Lamellipodia are cytoplasmic protrusions, which are formed at the leading edge of spreading or migrating cells to extend the cell (Lamalice et al., 2007). The formation of lamellipodia is associated with the Rac complex (Lamalice et al., 2007). Stress fibers are actin filaments of inverted polarity. They are linked by alpha-actinin and myosin, and distributed along contractile fibers. Stress fibers mediate cell body contraction, allowing the cell to move forward (Lamalice et al., 2007).

Recently, studies have reported that exosomes play a role in enhancing endothelial cell migration in ischemic models. The Hu group studied the role of induced- mesenchymal stem cells derived-exosomes (iMSCs- Exo) on HUVECs migration using an *in vitro* ischemia model. Their findings showed a significant increase in HUVEC migration after iMSCs-Exo treatment (Hu et al., 2015). Another study examined the migratory ability of human endothelial (EA.hy926) cells after treatment with mesenchymal stem cells derived-exosomes (MSC-Exo). Results show a significant enhancement of the migration of the EA.hy926 cells after 12 hrs of incubation with MSC-Exo (Zhang et al., 2015)

1. 3. 4. Extracellular vesicles and cellular uptake mechanism:

At the last stage of exosome biogenesis, exosomes are formed from the infusion of MVBs into the cell membrane. Furthermore, the exosome composition depends on the parent cells and their cytoplasmic components, which differentiates exosomes derived from different cells (Farooqi et al., 2017). Besides, it has been found that the composition of exosomes contains various materials such as proteins, mRNA, and miRs (Farooqi et al., 2017). Therefore, several studies indicated that exosomes can transfer mRNA and miRs horizontally(György et al., 2011). In addition, exosome internalization

leads to transfer of their cargo and exertion of their functions (e. g. antigen presentation) on the recipient cells: i) direct contact between vascular surface molecules and cells, ii), fusion into cell membrane, and iii) endocytosis of vesicles (Delenclos et al., 2017; György et al., 2011). Endocytosis can be mediated via different mechanisms. Examples of these mechanisms include phagocytosis, macropinocytosis, and clathrin-mediated endocytosis (Tian et al., 2014). Exosome uptake by the recipient cells occurs by receptor-mediated endocytosis, where molecules (e.g. proteins) on the exosome membrane surface interact with complementary molecules presented on recipient cell surface membrane, and then exosomes are internalized (Farooqi et al., 2017). Tian et al. detected the DiD-labelled exosomes isolated from rat pheochromocytoma PC12 cells in bone marrow-derived mesenchymal stromal cells (BMSCs). Exosomes were internalized via clathrin-mediated endocytosis and macropinocytosis, determined after treating BMSCs with 3 different chemicals: CPZ (to inhibit clathrin-mediated endocytosis pathway), EIPA, and LY294002 (to block macropinocytosis) (Tian et al., 2014). Moreover, they reported that PC12-derived exosomes transferred miR-21 into BMSCs successfully (Tian et al., 2014). In previous studies, we incubated HUVECs with PKH26-labelled exosomes for 3 hrs, and then we detected the labelled exosomes in the cell

cytoplasm. To determine the exosome uptake pathway, we blocked macropinocytosis by treating HUVECs with 10μM of EIPA prior to addition of PKH26-labeled exosomes. Exosomes uptake was dramatically decreased by EIPA (Viñas et al., 2016). Furthermore, in our lab, in a co-culture of ECFCs and HUVECs, we found that ECFC-derived exosomes entered HUVECs and delivered miR-486-5p into the cells (Viñas et al., 2016).

1. 4. MicroRNA and AKI:

MicroRNAs (miRNAs) represent a class of short single-stranded RNAs containing between 18 and 22 nucleotides (Gulyaeva and Kushlinskiy, 2016). MicroRNAs play a critical role in the regulation of gene expression at a posttranscriptional level by suppressing target mRNA, and blocking protein translation by interacting with the 3' untranslated region (UTR) of the target mRNA (Gulyaeva and Kushlinskiy, 2016). Interestingly, one gene can be regulated by many miRNAs, and one miRNA can regulate multiple genes (Jung and Suh, 2014). The mature miRNA is transcribed initially in the nucleus as primary-miRNA (pr-miRNA), then split by the enzyme Drosha to form precursor miRNA (pre-miRNA). It is then exported from the nucleus to the cytoplasm as mature miRNA (Jung and Suh, 2014).

Several studies reported that EVs carry a selective package of small RNAs with miRNA occupying the major population. These particular miRNA are transferred from the donor cell to neighboring cells through the derived vesicles (exosomes or MPs) to regulate protein expression in the recipient cells (Viñas et al., 2016). Several studies have assessed the therapeutic potential of miRNA in ischemic diseases. For example, a study performed on AKI demonstrated that the depletion of miR-126 and miR-296 from EVs, derived from human EPCs, attenuates renal repair *in vivo,* and reduces antiapoptotic effects *in vitro*. Another study indicates that a global downregulation of miRNA, from EV derived-mesenchymal stromal cells via Drosha knockdown, inhibits renal recovery (Collino et al., 2015).

Our lab found that ECFC-derived exosomes are highly enriched with miR-486-5p, which targets the phosphatase and tensin homolog (PTEN) and the Akt pathway (Viñas et al., 2016). We also found that hypoxic endothelial cells which were incubated with ECFC-derived exosomes, exhibited an increase in miR-486-5p, inhibition of PTEN, enhanced Akt phosphorylation, and decreased apoptosis (Viñas et al., 2016). Accumulating evidence suggests that infusion of ECFC-derived exosomes into mice with renal ischemia/reperfusion reduced renal injury via transfer of miR-486-5p, with targeting of PTEN, and increased Akt expression. However, when miR-486-

5p was silenced in exosomes, the protective effects were not observed in AKI mice. Taken together, these findings suggest that exosomes enriched in miR-486-5p may be a potential treatment method for ischemic AKI (Viñas et al., 2016).

1. 5. Summary of rationale

Many AKI studies show that stem cell or progenitor cell engraftment is not required to protect renal cells against ischemia. Rather, paracrine factors (e.g. exosomes) could be explored for their therapeutic potential in AKI. Several studies support the high proliferative capacity of ECFCs, and the beneficial role of released exosomes when infused into ischemic tissues. On the other hand, the *in vivo* studies suggested that ECFC-EVs might inhibit endothelial cell growth. Therefore, we sought to determine if ECFC-derived exosomes and MPs separately stimulate endothelial cell proliferation. In addition, ECFC-derived exosomes are enriched in miRNA 486-5p, which seems to play a role in protecting renal tissues against ischemia.

Moreover, the role of ECFC-derived exosomes/MPs and miRNA-486-5p on endothelial proliferation and cell migration has not yet been investigated in a model of ischemia. Furthermore, the mechanism of ECFC- derived exosome uptake by endothelial cells has not yet been investigated

intensively. In this study, I explored the effects of ECFC-derived exosomes and MPs, in addition to miRNA 486-5p, on renal endothelial cell proliferation and migration in a hypoxia/reoxygenation model. In addition, I examined the uptake pathway of ECFC-derived exosomes by renal endothelial cells (RECs) and human umbilical vein endothelial cells (HUVECs).

1. 6. Hypothesis:

1. ECFC-derived exosomes will stimulate endothelial cell proliferation and migration, while MPs will have the opposite effect.
2. ECFC-derived exosomes will internalize into endothelial cells via the macropinocytosis pathway.
3. MiRNA-486-5-p from human cord blood ECFC-derived exosomes will enhance endothelial cell migration.

1. 7. Objectives:

The aims of this study were:

1. To determine the effect of specific types of EVs (exosomes, and MPs) on renal endothelial cell proliferation and migration after hypoxia/reoxygenation (H/R) *in vitro*.
2. To examine the possible pathways of ECFC-derived exosome uptake by endothelial cells.
3. To examine the effect of MiR-486-5p on endothelial cell migration.

Chapter 2: Materials and Methods

2. 1. Cell culture

Renal Endothelial Cells (RECs) (Cell Biologics, Chicago, IL, USA) were cultured in Complete Endothelial Medium (Cell Biologics) with 10% Fetal Bovine Serum (FBS) (Wisent Bioproducts, St. Bruno, QC, Canada) in dishes pre-coated with 1% gelatin. Human umbilical vein endothelial cells (HUVECs) and human umbilical cord blood endothelial colony forming cells (ECFCs) were cultured in Endothelial Basal Medium-2 (EBM-2, Lonza, Mississauga, ON, Canada) supplemented with 10% FBS. Cells were grown at 37°C in humidified air with 5% CO_2.

HUVECs were obtained from the American Type Culture Collection (Manassas, VA)(Viñas et al., 2016). ECFCs were isolated from human umbilical cord blood. The ECFC isolation protocol was performed at The Ottawa Hospital (Ottawa, ON, Canada) after informed written consent and with approval from the institutional research ethics board. Briefly, ECFC were isolated from human umbilical cord blood- derived mononuclear cells, which were isolated by Ficoll density gradient centrifugation (Sun et al., 2013). Isolated ECFCs were cultured in endothelial basal media -2 (supplemented with SingleQuot supplements (Lonza, Basel, Switzerland),

10% FBS, and 1% 10,000 U/mL penicillin/10,000 mg/mL streptomycin/25 mg/ mL amphotericin), then incubated at 37 ^{o}C, 5% CO_2, in a humidified incubator. After the incubation period, ECFCs were detached using trypsin-Ethylenediaminetetraacetic acid (EDTA), washed twice in phosphate-buffered saline (PBS), and resuspended in 10% dimethyl sulfoxide (DMSO) for storage at -80°C (Burger et al., 2015). ECFC were characterized with CD31 and vascular endothelial growth factor receptor 2 (VEGFR2) by Flow cytometery and they were highly expressed (Burger et al., 2015).

2. 2. Exosome (EX) and Microparticle (MP) isolation

Conditioned ECFC media supplemented with 10% exosome-free FBS (Exosome–depleted FBS, System Bioscience, MountainView, CA, USA) was collected after 24 – 48 hrs of incubation with ECFC. Exosomes and MPs were isolated using differential centrifugation; which involved a low-speed (2,500 x g) centrifugation for 10 min to discard apoptotic bodies and dead cells (Fisher Scientific, Accuspin TM 400 centrifuge, Ottawa, ON, Canada). MPs were isolated from the remaining supernatant after being subjected to centrifugation, at 10,000 x g for 30 min at 4°C (Sorvall ® RC6 plus, Thermo, Waltham, MA, USA). Next, for exosome isolation, ultracentrifugation was performed at 100,000 x g for 90 min at 4°C,

(Beckman Coulter, Optima TM L 1 XP, Toronto, ON, Canada), Once re-suspended in PBS, the pellet was subjected to additional ultracentrifugation with the previous setting for additional purification. The pellet, containing exosomes, was either re-suspended in 100 µl of FBS-free media (for cell treatments), PBS (for nanoparticle tracking analysis), or radioimmunoprecipitation assay buffer (RIPA) (for western blot analysis), and stored at -80^{o}C.

2. 3. Nanoparticle tracking analysis

Extracellular vesicle (EV) size was measured using the Nanosight LM10 instrument (NanoSight Ltd., Amesbury, UK). Exosomes/MPs (6 µg/ml) were suspended in 500 µl of ice-cold PBS, and vesicle size was measured using Nanosight 2.7 software. A shutter speed of approximately 30 milliseconds was used with a camera gain between 250 and 650, and some analyses were done using the Zeta view device with shutter speed 2 seconds from 11 camera positions (Particle matrix, Meerbusch, Germany).

2. 4. Endothelial cell markers

In order to characterise REC or HUVEC expression of endothelial markers, cells were seeded in 6-well plates with coverslips, and incubated until 80-90% confluence. Cells were washed twice with sterile PBS, and

then treated with 10% bovine serum albumin (BSA) for 30 min at room temperature, followed by treatment with either a rabbit IgG antibody (Ab) targeting CD31 (Santa Cruz, Dallas, TX, USA) (1:100 in BSA), or goat IgG antibody targeting CD144 (Anti VE cadherin Ab, Santa Cruz) 1:100 in BSA. Control (CTL) cells were stained with secondary IgG Ab only. Cells were incubated with the primary antibodies overnight at 4°C in a humidified chamber, and then washed with PBS. Cells were then incubated with the appropriate secondary IgG antibody (anti-rabbit for CD31, or anti-goat for CD144) (1:100 in BSA, Jackson ImmunoResearch, West Grove, PA, USA) for 1 hr at room temperature. The washing step was repeated, followed by a Hoeschst 33342 staining step (1:2000 in distilled water (DW) for 3 min at room temperature). Endothelial cell markers were then visualized by microscopy (Axiovert 200M microscope, ApoTome.2, Zeiss, Toronto, ON, Canada).

2. 5. Immunoblotting

Following isolation, exosomes and MPs were re-suspended in 100 µl of RIPA buffer for detection of Tumor susceptibility gene 101 (TSG101). Exosomes and MPs were lysed in RIPA for 5 min at room temperature, followed by centrifugation at 12,000x g for 5 min at 4 ^{o}C to discard debris. The protein concentration was then measured using the (detergent

compatible) DC Protein assay (Bio-Rad, Mississauga, ON, Canada). Samples were boiled at 100 ^{o}C for 5 min, then equal amounts of protein (10 μg) were run on 10% sodium dodecyl sulfate polyacrylamide gels (SDS-PAGE) for 1 hr at 150 volts. Pre-stained standard (Precision plus protein dual colour standards, Bio-Rad) was used as a molecular weight marker. Once separated, the proteins were transferred to nitrocellulose membranes (Bio-Rad) for 1 hr at 100 volts. Membranes were then blocked with 5% skimmed milk in Tris-buffered saline and 0.1% Tween 20 (TBS-T) for 1 hr at room temperature. Next, membranes were incubated with mouse monoclonal anti-TSG101 antibody (1:2000; Abcam Inc., Toronto, ON, Canada) overnight at 4 ^{o}C with constant shaking. After incubation with primary antibodies, the membrane was washed with TBS-T for 5 min, three times, incubated with horseradish peroxidase conjugated secondary anti-mouse antibodies (1:2000, Jackson ImmunoResearch) for 1 hr at room temperature, then washed three times with TBS-T for 5 min each. Chemiluminescence (ECL; GE Health Care Bio-Science, Baie d'Urfe, Quebec, Canada) was used to detect proteins. In order to normalize the blots, antibodies targeting glyceraldehyde 3-phosphate dehydrogenase (GAPDH) (1:1000, Millipore, Toronto, ON, Canada) were used as a loading control.

Immunoblots were then developed on film (Raytech SRX-101, Konica Minolta, Mississauga, ON, Canada).

2. 6. 5-bromo-2'-deoxyuridine (BrdU) cell proliferation assay

Newly synthesized DNA was examined by measuring incorporation of 5-bromo-2'-deoxyuridine (BrdU) (Cell Proliferation ELISA, BrdU (colorimetric), Roche, Laval, Quebec, Canada) into REC and HUVECs in normoxic and hypoxic conditions.

In normoxia**,** $1x10^4$ cells/well (HUVECs or RECs) were seeded in a 96-well plate and incubated at 37 ^oC overnight. Then, the media was replaced with either 50 μg/ml of exosomes, 50 μg/ml of MPs, or 100 μl of ECFC-conditioned media (CM). Cells were incubated for 24 hrs and labeled with a 10 μM solution of BrdU. Cells were then incubated at room temperature in a product called fixdenat (FixDenat, Cell Proliferation ELISA, BrdU (colorimetric), Roche, Laval, Quebec, Canada) wherein cells are fixed and DNA denatured in one step for 30 min, followed by 90 min at room temperature with Anti-BrdU antibody (1:100). Next, the cells were incubated at room temperature for 10 min with substrate (tetramethyl-benzidine (TBM)) then analysed using an enzyme-linked immunosorbent assay (ELISA) microplate reader at wavelength 340-450 nm.

For hypoxia/reoxygenation (H/R) experiments, HUVECs/RECs were cultured onto 96-well plates overnightat 37 ºC. After incubation with freshly prepared media, with or without 10% FBS-free exosomes, cells were then incubated at 37 ºC for 24 hrs in a hypoxic chamber (Whitley H.5 hypoxystation, Don Whitly Scientific, Frederick, MD, USA) (1% O_2, 5% CO_2, 94% N_2, and 77% relative humidity). Media was replaced with fresh media, and the cells were treated with either 50 μg/ml of exosomes, 50 μg/ml of MPs, or 100 μl of ECFC-conditioned media (CM). Then, cells were incubated in normoxic conditions (reoxygenation) for an additional 24 hrs. The BrdU assay was then performed as outlined above. All experiments were performed in duplicate.

2. 7. 5-ethynyl-2'-deoxyuridine (EdU) staining

RECs/HUVECs were cultured in 6-well plates with coverslips and incubated overnight, then treated with 7.5 μg/ml of exosomes for 24 hrs. Cells were then labeled with 10 μM of 5-ethyl-2`-deoxyuridine (EdU) (Click-iT® Plus EdU Alexa Fluor® 488 Imaging Kit, Life Technologies, Grand Island, NY, USA) for two hrs (HUVECs) or 16 hrs (RECs) depending on the cell growth rate. Next, cells were fixed with 3% paraformaldehyde for

15 min at room temperature. Then, the fixative solution was washed twice with one mL of 3% BSA in PBS. Cells then were incubated at room temperature with 1 mL of 0.5% Triton® X-100 (Click-iT® Plus EdU Alexa Fluor® 488 Imaging Kit, Life Technologies) for 20 min for permeabilization. Cells were washed twice with 3% BSA in PBS. Then, for EdU detection, cells were incubated for 30 min at room temperature (protected from light) with 0.5 ml of reaction cocktail (440 µl of 10% reaction buffer, 10 µl of copper protectant, 1.2 µl of Alexa Fluor picolyl azide, and 50 µl of 10% additive buffer) (Click-iT® Plus EdU Alexa Fluor® 488 Imaging Kit, Life Technologies). Then, cells were washed twice with 3% BSA in PBS, and stained with Hoechst (1:2000 in PBS) for 3 min. Finally, samples were examined for newly synthesized DNA using an Axiovert 200M microscope (ApoTome.2, Zeiss, Toronto, ON, Canada).

2. 8. Exosome uptake studies

In order to study exosome uptake pathways, exosomes were labeled with the red fluorescent dye PKH26 (Cell Linker Kits, Sigma-Aldrich, St. Louis, MO, USA). Briefly, after exosomes were isolated from ECFC CM, they were re-suspended in a solution containing 250 µl of a product called reagent C diluent (Cell Linker Kits) and 1 µl of PKH26 dye, then incubated

for 5 min at 37 °C in the dark. The staining reaction was then stopped by incubating the exosomes in 500 µl of media supplemented with 10% FBS-depleted exosomes, for one minute. Finally, labeled exosomes were subjected to ultracentrifugation (as described above) for washing and the labeled exosomes were re-suspended in 100 µl media free-FBS for cell treatment in uptake studies.

RECs were cultured in 12-well plates with 18 mm coverslips and, incubated at 37 °C until they reached 70% confluence in 48 hrs, Cells were pre-treated with either of the following pharmacological inhibitors: 10 µM ethyl-isopropyl amiloride (EIPA), 1, 5, or 10 µM Chlorpromazine (CPZ) (Sigma-Aldrich), or 10, 20, or 50 µM LY294002 (Sigma-Aldrich), for 30 min at 37 °C. Cells were then incubated with labeled exosomes for 3-4 hrs at 37 °C. Control cells were incubated with labeled exosomes for 3-4 hrs in the absence of inhibitors. After washing cells twice with sterile PBS at room temperature, they were fixed with two mls of 3% paraformaldehyde for 20 min. Cells were blocked with two mls of 1% cold BSA for 20 min, then stained with Phallodin 488 (green) (Phallodin molecular probes, Invitrogen, Carlsbad, CA, USA) (1:2000) for 20 min at room temperature, in the dark. Cells were then stained with Hoechst 33342 (1:2000 in PBS) for 3 min. Internalized exosomes were then counted using confocal microscopy

(Axiovert 200M microscope, ApoTome.2, Zeiss, Toronto, ON, Canada). The numbers of PKH-positive exosomes from 6 fields were counted per high power field and averaged from each coverslip, in a blinded fashion.

2. 9. Cell transfection

RECs/HUVECs were seeded onto 96-well plates and then transfected with pre-miR-486-5p using Lipofectamine according to the manufacturer's instructions, with some modifications. Briefly, 1.5 μl of Lipofectamine RNAiMAX reagent (Life Technologies) was diluted in 25 μl of a product called Opti-MEM media, followed by the addition of either scrambled RNA or pre-miR-486-5p (0.5 μl (5 pmol)), with 5 min of incubation (room temperature). Media was then replaced with 90 μl of freshly prepared media plus 10 μl (1 pmol) of the RNA complex, and cells were incubated for 24 hrs at 37 ^{o}C.

2. 10. MicroRNA isolation and real-time polymerase chain reaction (PCR)

In order to evaluate the quality of transfections, total RNA fractions (containing microRNA) were extracted using the miRNeasy Mini Kit (Qiagen Inc., Toronto, ON, Canada) from cells grown on 96-well plates. Four experimental groups were studied, with each assay performed in

quadruplicate: i) control (cells + media with 10% FBS), ii) cells transfected with pre-miR-486-5p (Life Technologies, Inc.), iii) cells transfected with scrambled RNA, and iv) cells with Lipofectamine alone. 24 hrs after transfection, the media was discarded. Cells were washed two times with PBS, and then lysed with 100 µl of a product called Qtryzol lysis solution (miRNeasy Mini Kit, Qiagen Inc, Canada). RNA concentrations were measured using Bradford assay. 2 µl of the extracted RNA were diluted in 500 µl of double distilled water. Then, the RNA concentration was measured via spectrophotometer (Spectronic genesis 5, Spectronic Instruments, Rochester, NY, USA). The experimental groups were divided into four groups; i) control (CTL); cell only, ii) transfected cell with pre–miR-486-5p, iii) scrambled RNA, and iv) Lipofectamine only. The following steps were done according to the manufacturer. TaqMan MicroRNA Reverse Transcription Kit (100mM dNTPs, 50 U/μL MultiScribe™ Reverse Transcriptase, 10× reverse transcription buffer, 20 U/μL RNase Inhibitor, and nuclease-free water) (Life Technologies, Inc.) was used for cDNA preparation. For real-time PCR, 20X mir-486-5p and 20X U6 primers were used (Taqman MicroRNA assays, Applied Biosystems, Thermofisher Scientific, Foster City, CA, USA) and the real-time PCR reactions were performed in an Applied Biosystems 7000 sequence detection real-time PCR

system (Thermofisher Scientific). Mamm-U6 RNA was used to normalize differences in RNA levels for each sample. The relative amount of miRNA to U6 RNA was expressed using the 2 DDCt method (Viñas et al., 2016).

2. 11. Cell migration

RECs or HUVECS were seeded onto 96-well plates, and incubated until confluent. The media was then replaced with freshly prepared media with either FBS-free media, or media with 10% FBS- exosomes free. Cells were then subjected to either normoxia or hypoxia (1% O_2, 5% CO_2, 94% N, and 77% relative humidity) for 24 hrs at 37 ^oC before being scratched using WoundMaker (Essen BioScience, Ann Arbor, MI, USA). After scratching, cells were washed twice with PBS, and suspended in media loaded with 50 μg/ml of either exosomes or MPs. Images were taken by InCucyte (Essen BioScience) every two hours for 24 to 48 hrs at 37 ^oC and 5% CO_2, and images were analysed using ImageJ by measuring the wound area using freehand tool.

2. 12. Statistical analysis

All experiments were performed at least three times. The data are expressed as the mean ± standard error, and were analyzed using one-way analysis of variance, with a Bonferonni post-test as appropriate. All statistical analyses were performed with Graphpad Prism version 7.0 (GraphPad Software, Inc., La Jolla, CA). $P < 0.05$ was considered as significant.

2. 13. Statement of Contributions

I have performed all the experiments and assays described in this thesis except for the following: 1) Dr. Alex Gutsol did the endothelial cell marker staining experiments. 2) The exosome uptake studies for HUVEC cells were conducted with the assistance of Dr. Jose Vinas.

Chapter 3: Results

3. 1. Cell and extracellular vesicle characterization

3. 1. 1. Characterization of endothelial cell markers:

In order to determine if RECs and HUVECs were expressing endothelial cell surface markers, RECs and HUVECs were stained with endothelial cell surface markers CD31 (red) and CD144 (green), located at cell-cell junctions (Lertkiatmongkol et al., 2016; Vestweber, 2008). Both cell lines expressed these endothelial markers **(Fig. 2),** confirming that each cell line of interest expressed the expected endothelial cell antigens. Negative controls (stained without primary Ab) demonstrated no expression of endothelial markers as a comparison group **(Fig. 2)**.

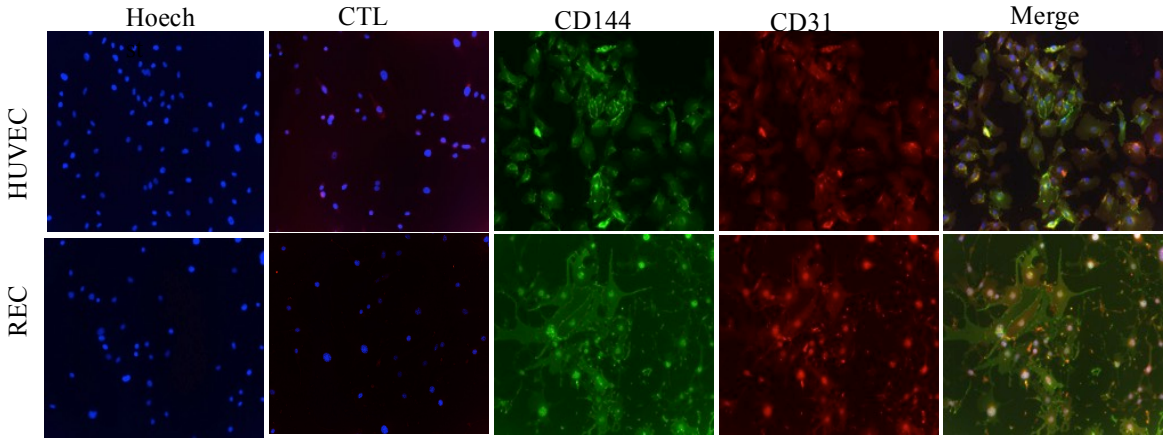

Figure 2. Renal endothelial cells express both endothelial cell markers CD31 and CD144. Renal endothelial cells (RECs) and Human umbilical vein endothelial cells (HUVECs) were cultured on 6-well plates and treated with the following: Hoechst (blue); nuclear stain, CTL; negative control (cells treated with secondary Ab only), CD144 (green) and CD31 (red) antibodies. Images are representative photomicrographs (N=3), magnification 200X .

3. 1. 2. Characterization of ECFC-derived exosomes and MPs

Western blots were performed to assess the purity of ECFC-derived exosomes and MPs, which were isolated by serial ultracentrifugation. Western blotting revealed the expression of the exosome marker TSG101 in ECFC-derived exosomes, while ECFC-derived MPs showed no expression of TSG101 (**Fig. 3A, N=5 for exosome, N=4 for MPs**). In addition, Nanoparticle tracking analysis was performed for the exosome and MP fractions, which revealed characteristic size distribution for each class of vesicles. Exosomes had a mean diameter of 138 nm (mode, 89 nm) with 81.0% within the size range of 40 to 100 nm. MPs had a mean diameter of 230 nm (mode, 104 nm) with 78.6% within the size range of 100 to 1000 nm. The representative tracings are shown in **Fig. 3B**(**N=5**).

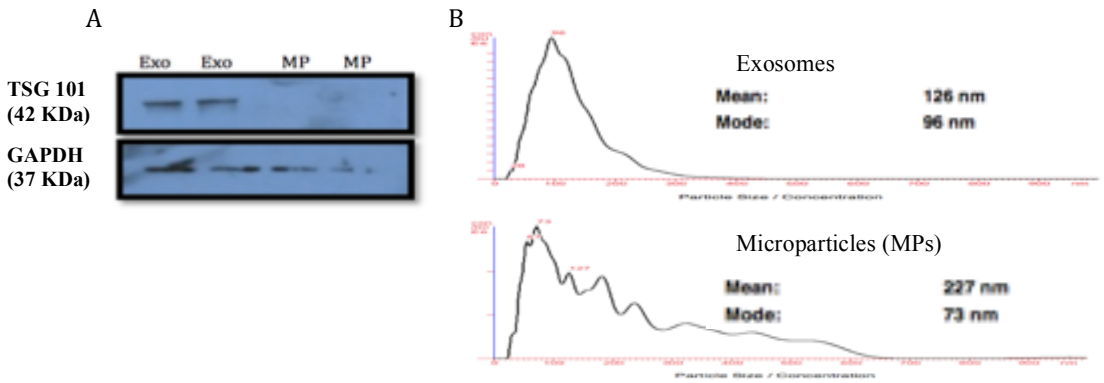

Figure 3: Characterization of ECFC-derived exosomes (Exo) and microparticles (MPs). A) Representative western blot (N=4-5) identifies exosome marker TSG101 in Exo, but not in MPs. **B)** representative Nanoparticle tracking analysis of exosomes (Exo, upper panel) and Microparticles (MPs, lower panel) isolated from ECFC-conditioned media. Exosomes had a mean diameter of 138 nm (mode, 89 nm) with 81.0% within the size range of 40 to 100 nm. MPs had a mean diameter of 230 nm (mode, 104 nm) with 78.6% within the size range of 100 to 1000 nm. Representative tracing is shown (N=5).

3. 2. Cell proliferation studies

3. 2. 1. REC proliferation results:

1. ECFC-derived exosomes and MPs promote REC proliferation in normoxia

To examine the effects of ECFC-derived exosomes and MPs on REC proliferation in normoxia using the BrdU assay, cells were treated with 50 μg/ml of exosomes or MPs for 24 hrs. Under serum-starved conditions, cell growth was significantly higher following treatment with either exosomes or MPs (**Fig. 4A; * p< 0.05 vs control (CTL; 0% FBS, n=8),** but not in the presence of FBS (**Fig. 4B).**

Next, we studied the effect of a lower concentration of exosomes (7.5 μg/ml) on REC proliferation in normoxia, using EdU staining. Under serum starved conditions, ECFC-derived exosomes did not change the degree of cell proliferation significantly. Furthermore, in the presence of serum condition, exosomes had no effect on EdU staining at this lower concentration. In addition, the presence of 10% FBS alone did not increase the number of proliferative cells in the EdU assay (**Fig. 5A, and B, n=3**).

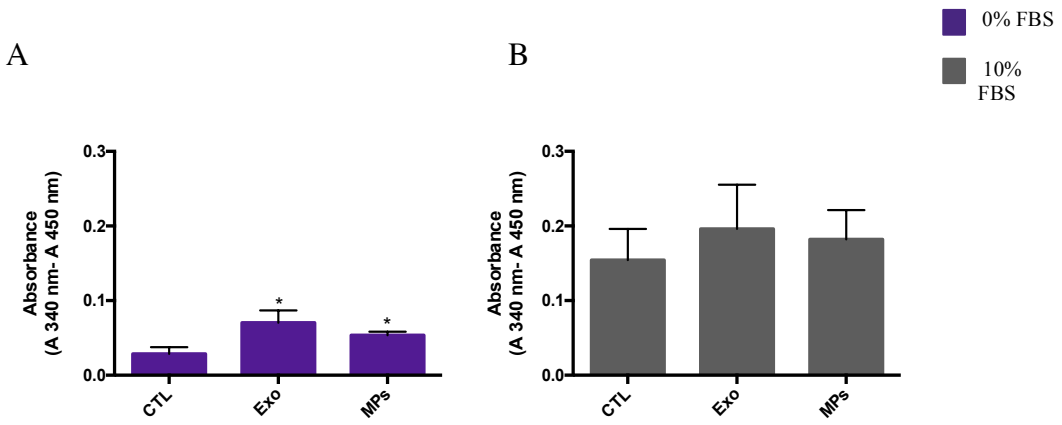

Figure 4. ECFC-derived exosomes (Exo) and microparticles (MPs) promote renal endothelial cells (RECs) proliferation in normoxia under serum starvation. Cells were grown on 96-well plates, then treated with 50 µg/ml of either ECFC-derived exosomes or MPs: **A)** without FBS, or **B)** with 10% FBS. Then, cells were incubated for 24 hrs in normoxia. **CTL;** control (cells only), **Exo;** exosomes, **MPs;** microparticles. Values are mean± SEM, * $p < 0.05$ vs. -----CTL; 0% FBS), n=8. Experiments were done in duplicate. Statistical significance was confirmed using one way analysis of variance (ANOVA).

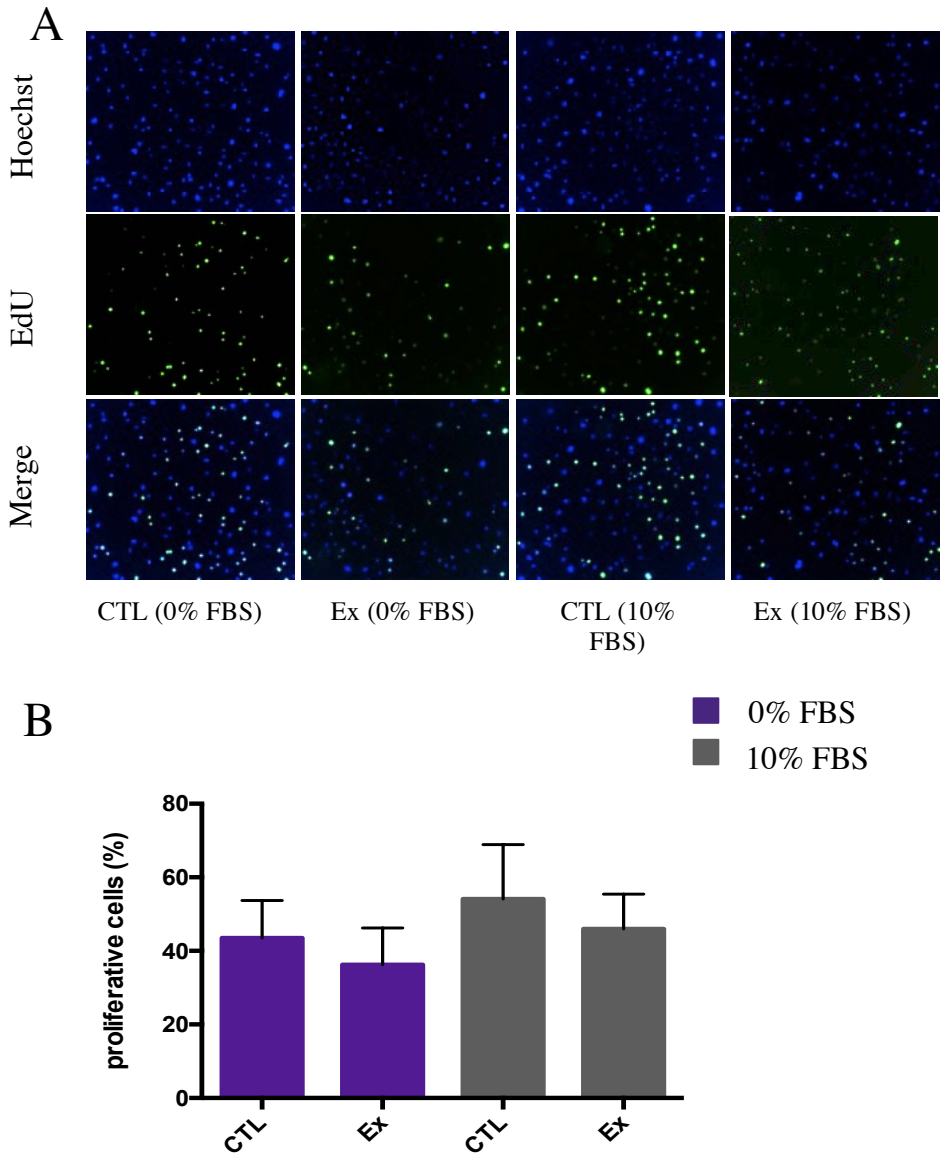

Figure 5. ECFC-derived exosomes at lower concentration has no effect on RECs proliferation in normoxia. Cells were incubated for 24 hrs with 7.5 µg/ml of exosomes and the proliferative cells detected by EdU staining. **A)** Representative photomicrograph of newly proliferating cells, Hoechst (blue), EdU (green). Magnification 200X. **B)** A bar graph illustrates the effect of 7.5 µg/ml of ECFC-derived exosomes on REC proliferation, n = 3.

3. 2. 1. 2. ECFC-derived MPs stimulate REC proliferation in hypoxia

After determining the effect of ECFC-derived exosomes and MPs on REC proliferation under the normoxic condition, we studied the impact of ECFC-exosomes and MPs on REC proliferation under hypoxic conditions (1% O_2).

RECs were subjected to hypoxic conditions for 24 hrs. Then, at the time of re-oxygenation, cells were treated with ECFC-derived exosomes (50 μg/ml), and MPs (50 μg/ml) and incubated for 24 hrs. Under serum-starved conditions, exosomes displayed a tendency to increase REC proliferation, although this was not statistically significant (**Fig. 6A, N=6**). However, MPs induced a significant increase in cellular proliferation * $p < 0.05$ vs. CTL (0% FBS) (**Fig. 6A, N=6**). In the presences of 10% FBS, when cells were treated with ECFC-derived exosomes, or MPs, cellular proliferation was not affected (**Fig. 6B, N=6**). In addition, when we treated RECs with ECFC conditioned media (CM) (100 μl) (which contain both exosomes and MPs) there was no change in cell proliferation (**Fig. 6B, N=6**).

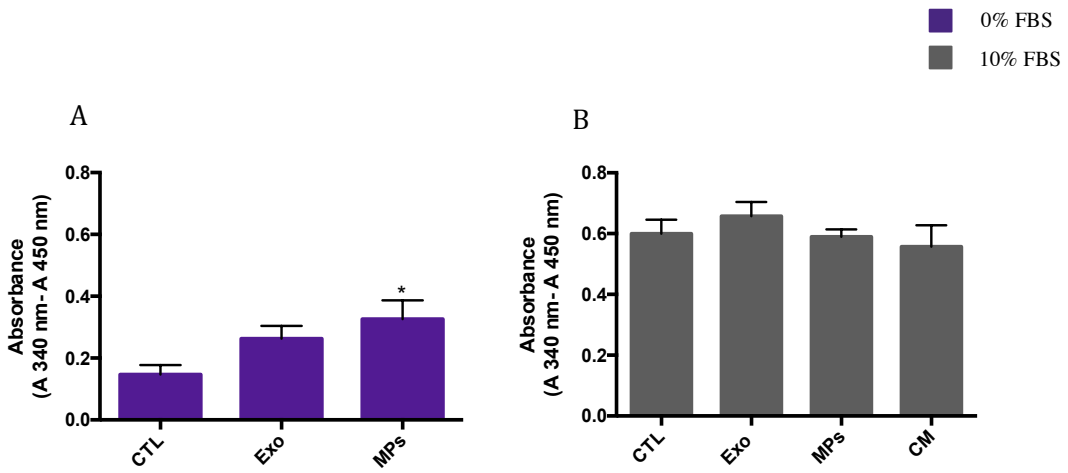

Figure 6. ECFC-microparticles (MPs) promote cell proliferation after hypoxia in RECs. Cells were subjected for 24 hrs to hypoxia, and at the time of re-oxygenation, **A)** cells were treated with 50 μg/ml of either exosomes (**Exo**) or **MPs** under serum starvation. **B) at the time of re-oxygenation,** cells were treated with the same concentrations of Exo, MPs, or ECFC conditioned media (**CM**) in the presence of 10% FBS. As control (**CTL**) cells were treated with/without FBS. Values are means ± SEM, * $p < 0.05$ vs CTL (0% FBS) n=6. Experiments were done in duplicate. One-way analysis of variance (ANOVA) was used for the statistical analysis.

3. 2. 2. HUVEC proliferation results

3. 2. 2. 1. Effect of ECFC exosomes and MPs on HUVEC proliferation

After we explored the impact of ECFC-derived exosomes and MPs on REC proliferation, we determined the effect of these vesicles on HUVEC proliferation following the same protocol as we did for REC experiments.

To examine the effect of exosomes and MPs on cell proliferation, HUVECs were treated with 50 μg/ml of either ECFC-derived exosomes or MPs, then incubated for 24 hrs in normoxic conditions with/without 10% FBS. FBS caused a significant increase in cell proliferation (* $p < 0.05$ vs control (CTL 0% FBS). However, treatment with ECFC-derived exosomes (**Fig. 7A, n=7**) or MPs (**Fig. 7B, N=4**), with or without FBS, did not affect proliferation.

Next, HUVECs were subjected to a lower concentration of exosomes (7.5 μg/ml) to determine the impact of exosomes on HUVEC proliferation in normoxia, using EdU staining. In the presence or absence of FBS, exosomes have no significant effect on HUVEC proliferation (**Fig. 8, n=3**).

We then investigated the impact of ECFC-derived exosomes and MPs (both at 50 μg/ml) on HUVEC proliferation after 24 hrs of incubation under

H/R conditions. Although cellular proliferation tended to increase after the cells were treated with ECFC-derived exosomes and MPs under serum starvation, statistical significance was not achieved (**Fig. 9A**, **N=7**). In the presence of serum, ECFC-derived exosomes, MPs and conditioned media treatment did not change the degree of cellular proliferation. (**Fig. 9B, N=7**).

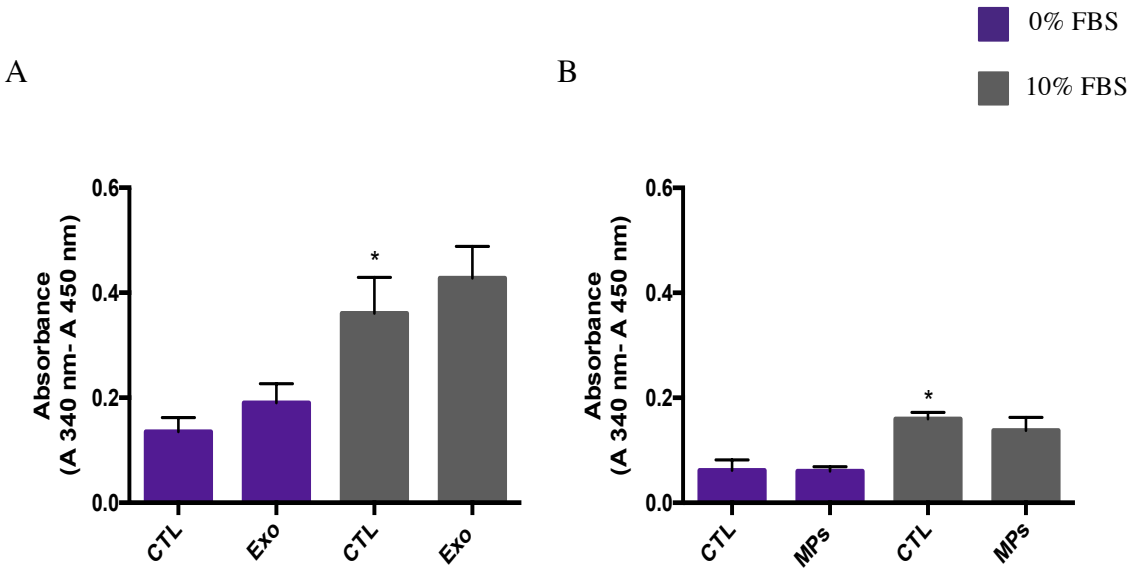

Figure 7. The effect of ECFC-derived exosomes (Exo) and microparticles (MPs) on HUVEC proliferation in normoxia. HUVECs were incubated with/without FBS and ECFC-derived exosomes (Exo, 50 μg/ml) (A), or microparticles (B) (MPs, 50 μg/ml), for 24 hrs and the new synthesized DNA was determined using BrdU assay. **CTL**; control (cells only). There was no significant effect of Exo or MPs on cell proliferation. Values are means ± SEM, * $p < 0.05$ vs control (CTL, 0% FBS) n=7 for exosomes, n=4 for MPs.

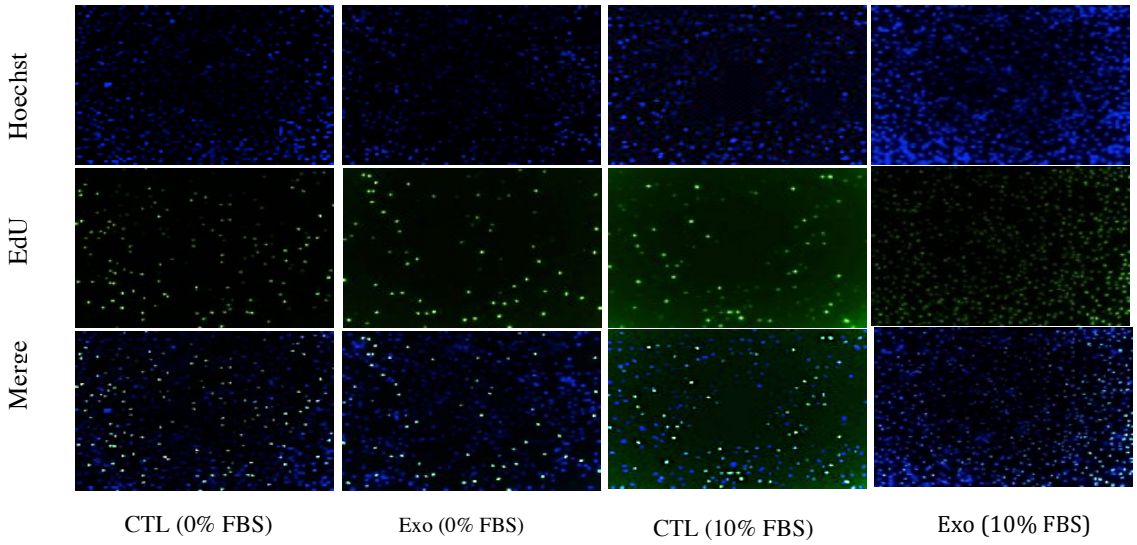

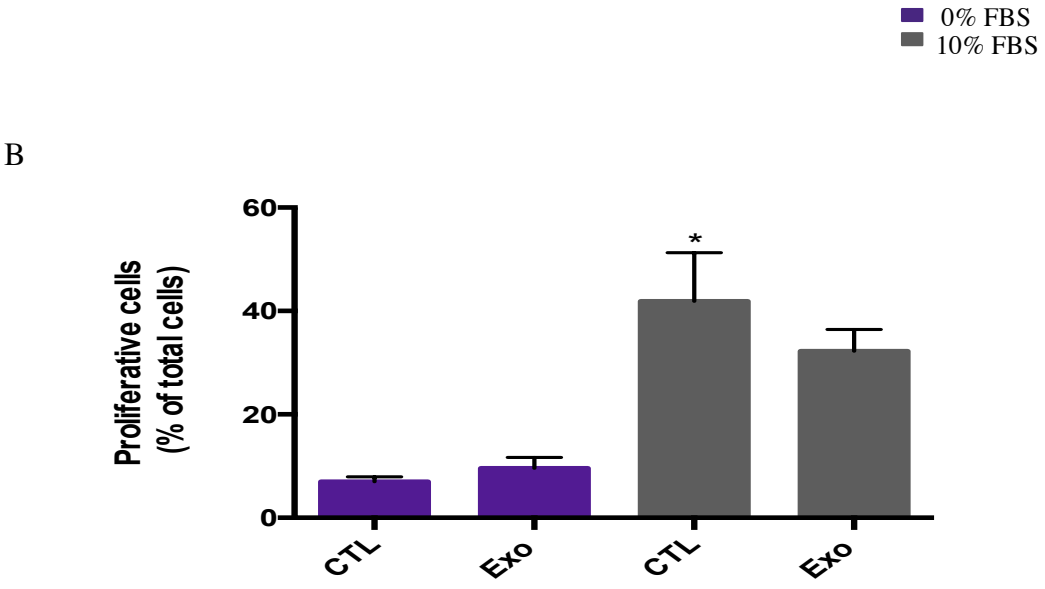

Figure 8. The effect of ECFC-derived exosomes on HUVECs proliferation in normoxia. Cells were incubated for 24 hrs with 7.5 μg/ml of exosomes and the proliferating cells detected by EdU staining. (A) Hoechst nuclear staining (blue), EdU (green), Merge shows both Hoechst and EdU stains. (B) Graph illustrating the effect of exosomes on HUVEC proliferation using EdU staining. Values are means ± SEM, * p <0.05 vs control (CTL, 0% FBS); n = 3. Magnification 200X

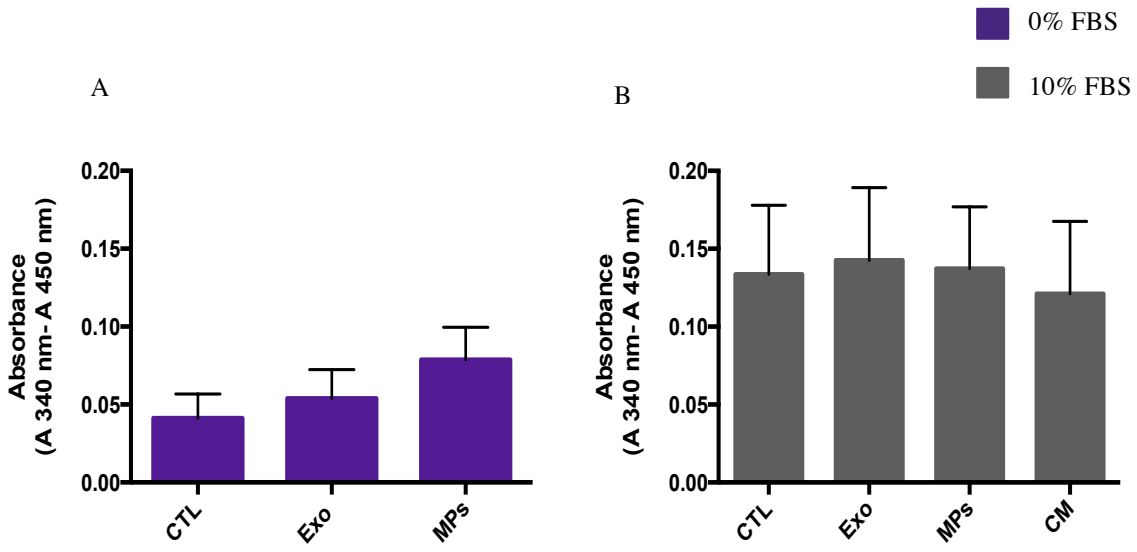

Figure 9. ECFC-derived extracellular vesicles and conditioned media (CM) have no effect on HUVECs proliferation in hypoxia. HUVECs were incubated in the presence or absence of ECFC-derived Exosomes (Exo) (50 μg/ml), microparticles -(MPs) (50 μg/ml), or conditioned media (CM) (100 μl), and cells were studied in A) 10% FBS, and B) 0% FBS. N=7.

3. 3. Exosome uptake studies

3. 3. 1. Uptake of ECFC- derived exosomes by REC

Recent studies suggest that exosomes can transfer their cargo contents from donor cells to the recipient cells by attaching or entering the cell in a process called endocytosis (Tian et al., 2014). Indeed, there are several pathways that mediate endocytosis such as macropinocytosis, and clathrin-mediated endocytosis (Tian et al., 2014). Previously, we reported that ECFC-derived exosomes can internalize into HUVECs via macropinocytosis. This was detected when we blocked macropinocytosis with 10 μM of EIPA for 3 hrs. Data showed a dramatic decrease in the exosomes uptake comparing to untreated HUVECs where we detected labeled exosomes in the cell cytoplasm (Viñas et al., 2016).

First of all, according to the previous findings, we examined the morphologic changes in RECs after ethylisopropyl amiloride (EIPA) treatment (10 μM) to ensure cell morphology was not affected by the treatment. Under normal growth conditions, endothelial cells are aligned longitudinally (Huang et al., 2013). This normal REC morphology is demonstrated in **Fig. 10, CTL; control**. After the cells were incubated for three hours with 10 μM of EIPA, cell morphology did not change. 10 μM of

EIPA was therefore used for further experiments, as it did not appear to induce cell death or apoptosis (**Fig. 10, N=4**).

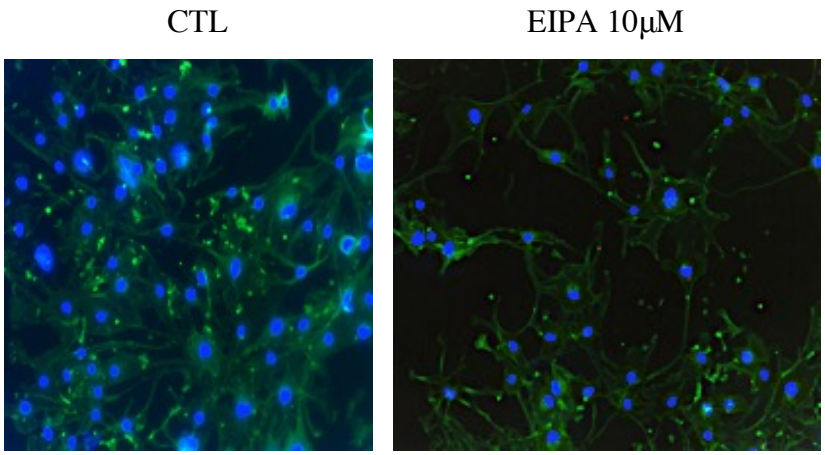

Figure 10. Incubation with EIPA did not change RECs morphology. Representative images of untreated RECs (**CTL;** Control). Cells treated with 10 μM of EIPA only (**EIPA 10 μM**). RECs were stained with phalloidin Alexa Fluor (green), nuclear counterstaining was performed using Hoechst (blue). N= 4. Magnification 200x.

To investigate possible pathways mediating exosome internalization into RECs, we subjected the RECs to different inhibitors (EIPA, CPZ, LY294002), each of which each block one of the endocytosis pathways (macropinocytosis, and clathrin-mediated endocytosis). As shown in **Fig. 11**, labelled exosomes were detected around the nucleus in RECs cytoplasm, and the inhibition of macropinocytosis using EIPA did not affect exosome uptake by the RECs (**Fig. 11A, and B, n=4**).

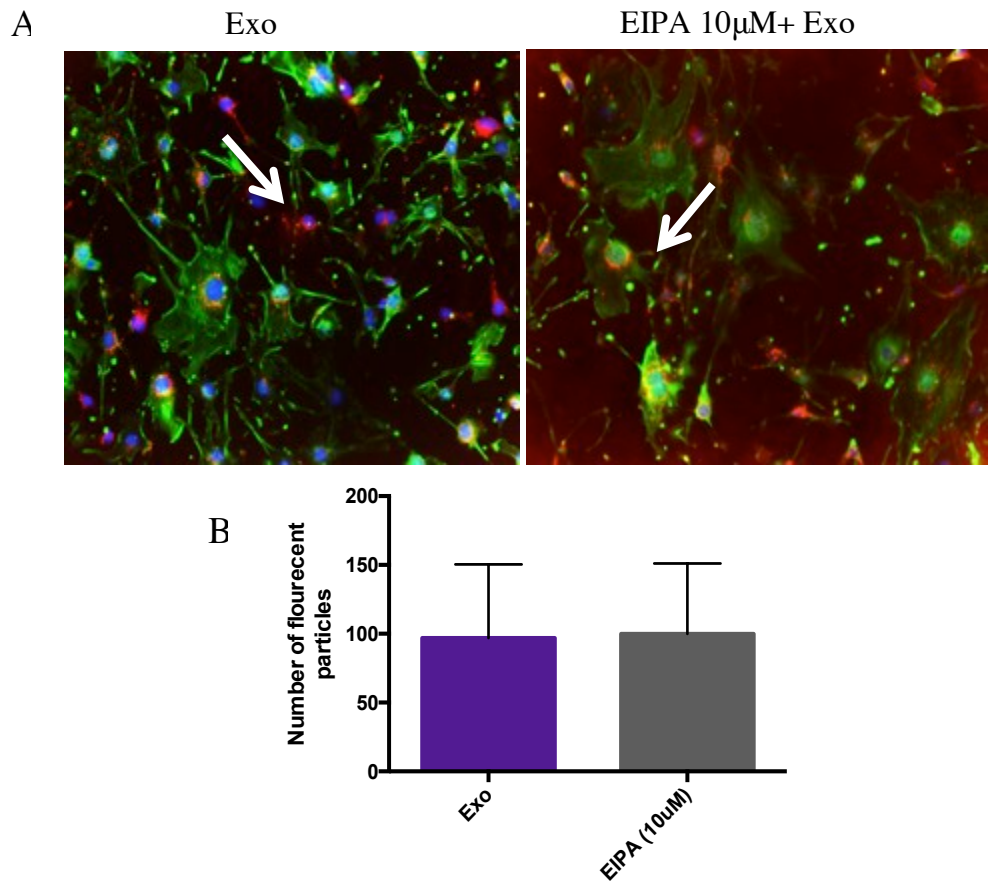

Figure 11. ECFC-derived exosome internalization by RECs was not blocked by EIPA. **A)** Representative microphotographs of RECs treated with exosomes only for comparison (**Exo**), and RECs pre-treated with 10 μM of EIPA and incubated for 4 hrs with ECFC-derived exosomes (**EIPA 10µM+ Exo**). RECs were stained with phalloidin Alexa Fluor (**green**), nuclear counterstaining was performed using Hoechst (**blue**), and exosomes were labeled with PKH26 (**red**). Magnification 200x. **B)** A graph illustrates that treatment with EIPA did not block exosome uptake by REC; n= 4. Arrows indicate exosome localization.

Next, we treated RECs with CPZ, which inhibits clathrin-mediated endocytosis, and LY29002, which blocks micropinocytosis (Tian et al., 2014). We used varying doses (LY294002; 10, 20, 50 μM, CPZ; 1, 5, 10 μM) to examine the relation between inhibitor concentration and exosome uptake. RECs were incubated with LY29002 and CPZ for 30 min at 37 ^{o}C, and then incubated with PKH26-labeled exosomes for 3 hrs at 37 ^{o}C, with inhibitors present throughout the experiment. As shown in **Figure 12A, B**, we observed that the uptake of labeled exosomes was lower than that of the control (Exo) for each concentration of both inhibitors. These results, however, were not statically significant for either of the treatments with LY294002 and CPZ (**Fig. 12A, B**). We then performed pooled analysis by combined the three different concentrations in one group for each treatment, and compare the pooled group to the control (exosomes only). The pooled groups showed a tendency to have a significant effect (LY294002 $p<0.02$ vs control (exosomes only), CPZ $p<0.04$ vs control (exosomes only).

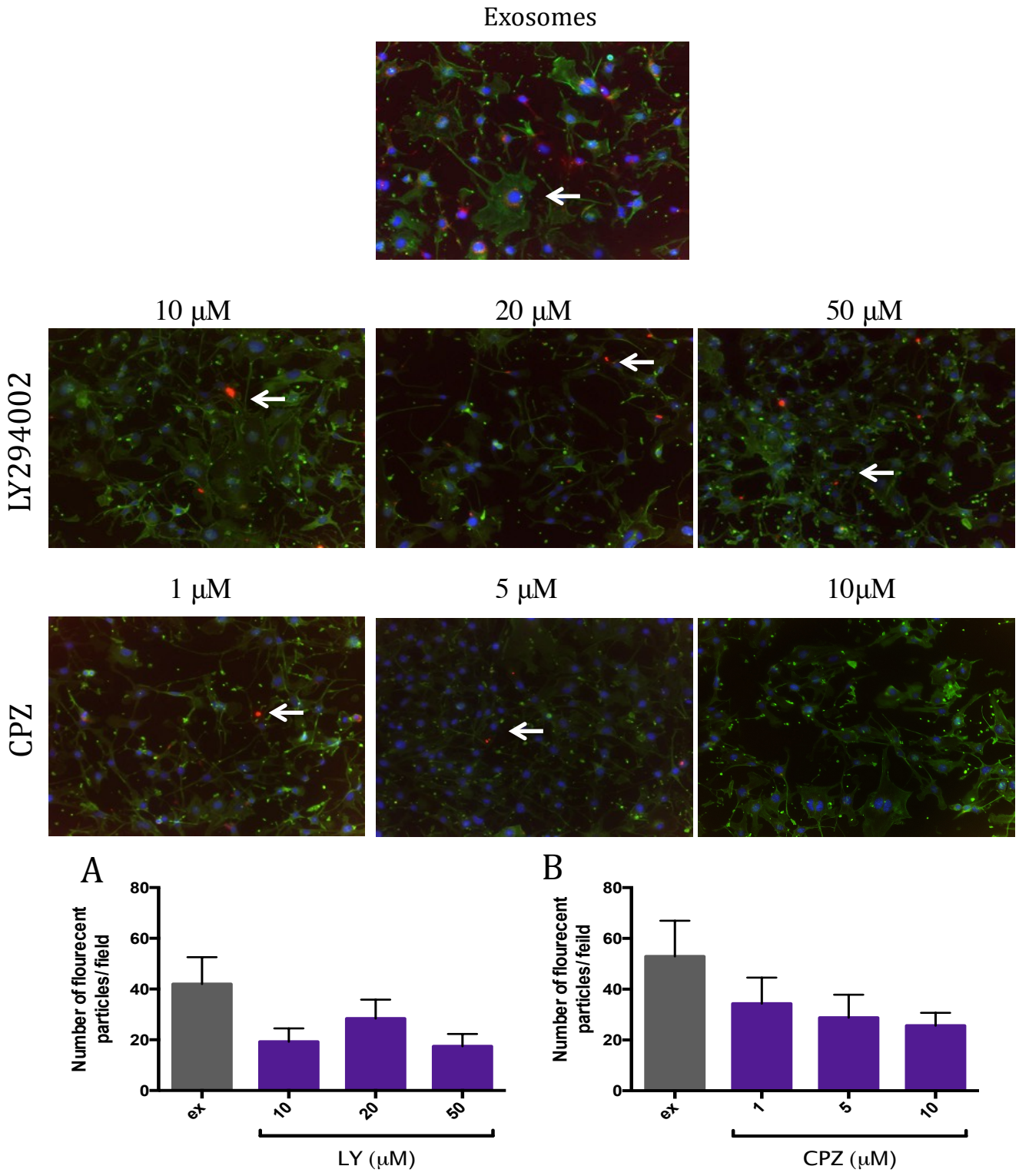

Figure 12. LY29004 and CPZ tend to block ECFC-derived exosome internalization by RECs. RECs were pretreated for 30 min with different concentrations of **A)** LY29004 and **B)** CPZ, and then cells were treated with PKH26-labeled exosomes for 3 hrs. **A)** Graph shows the number of labeled exosomes in RECs at 10, 20, and 50 μM of LY294002. **B)** Graph shows the number of labeled exosomes at 1, 5, and 10 μM of CPZ, n=7 CTL (exosomes only) representative image of exosomes for both treatments. Arrows indicate exosome localization Magnification 200x.

3. 3. 2. Uptake of ECFC-derived exosomes by HUVECs

To determine if ECFC-derived exosomes are taken up by HUVECs, we incubated the cells for 4 hrs with PKH26-labeled exosomes as shown in **Figure 13.** Exosomes were detected in the cytoplasm of the HUVECs (white arrows) (**Fig. 13B**). However, when we treated the cells with 10 μM EIPA, there was a dramatic decrease in the number of exosomes detected inside the HUVECs (**Figure 13C,** n=3).

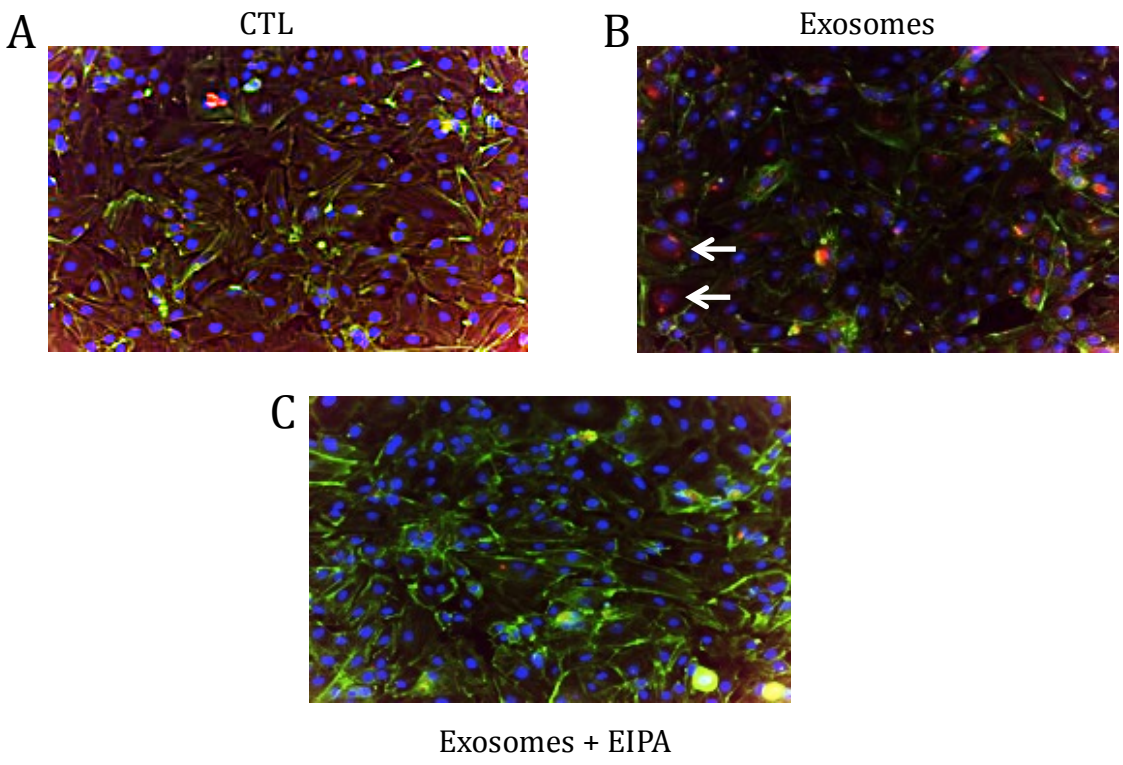

Figure 13: Internalization of ECFC-derived exosomes by HUVECs is blocked by EIPA. Representative images of HUVECs treated for 4 hours, with 20 μg/ml of ECFC-derived exosomes (Exosomes) --- compared with untreated HUVECs (CTL) and HUVECs pre-treated with 10 μM of EIPA (Exosomes+EIPA). HUVECs were stained with phalloidin Alexa Fluor (green), nuclear counterstaining was performed using Hoechst (blue), and exosomes were labeled with PKH26 (red). Arrows indicate exosome localization. Magnification 200x.

3. 4. Cell migration studies

3. 4. 1. ECFC-derived exosomes and MPs promote REC migration in normoxic conditions

In order to analyse whether the migratory capacity of RECs is affected by exosomes and MPs isolated from ECFCs, cells were incubated with ECFC-derived exosomes and MPs for 24 hrs.

Under serum-starved conditions, ECFC-derived exosomes increased REC migration significantly starting at the 20 hrs mark, and persisting to 48 hours. The wound, however, did not completely close after 48 hours of incubation (**Fig. 14A, and C, * p < 0.05, ** p <0.01, *** p < 0.001 vs. control (CTL), N=5 for exosomes**). ECFC-derived MPs caused an even higher increase in REC migration compared to exosomes at the 22 hrs mark, with the wound being partially closed **(+ p < 0.05 vs. control (CTL), N= 4 for MPs; Figure 14A**).

In the presence of FBS, treatment of RECs with exosomes after wound scratch significantly enhanced cell migration after 4 hours, resulting in wound closure in under 24 hrs (*** p < 0.05, ** p <0.01, *** p < 0.001 vs control (CTL), N= 5**) **(Fig. 14B).** MPs also caused a significant enhancement in cellular migration at eight hrs, resulting in wound closure in

less than 24 hrs as well **(+ p < 0.05, ++ p < 0.01, +++ p < 0.001 vs control (CTL), N=4) (Fig. 14B).**

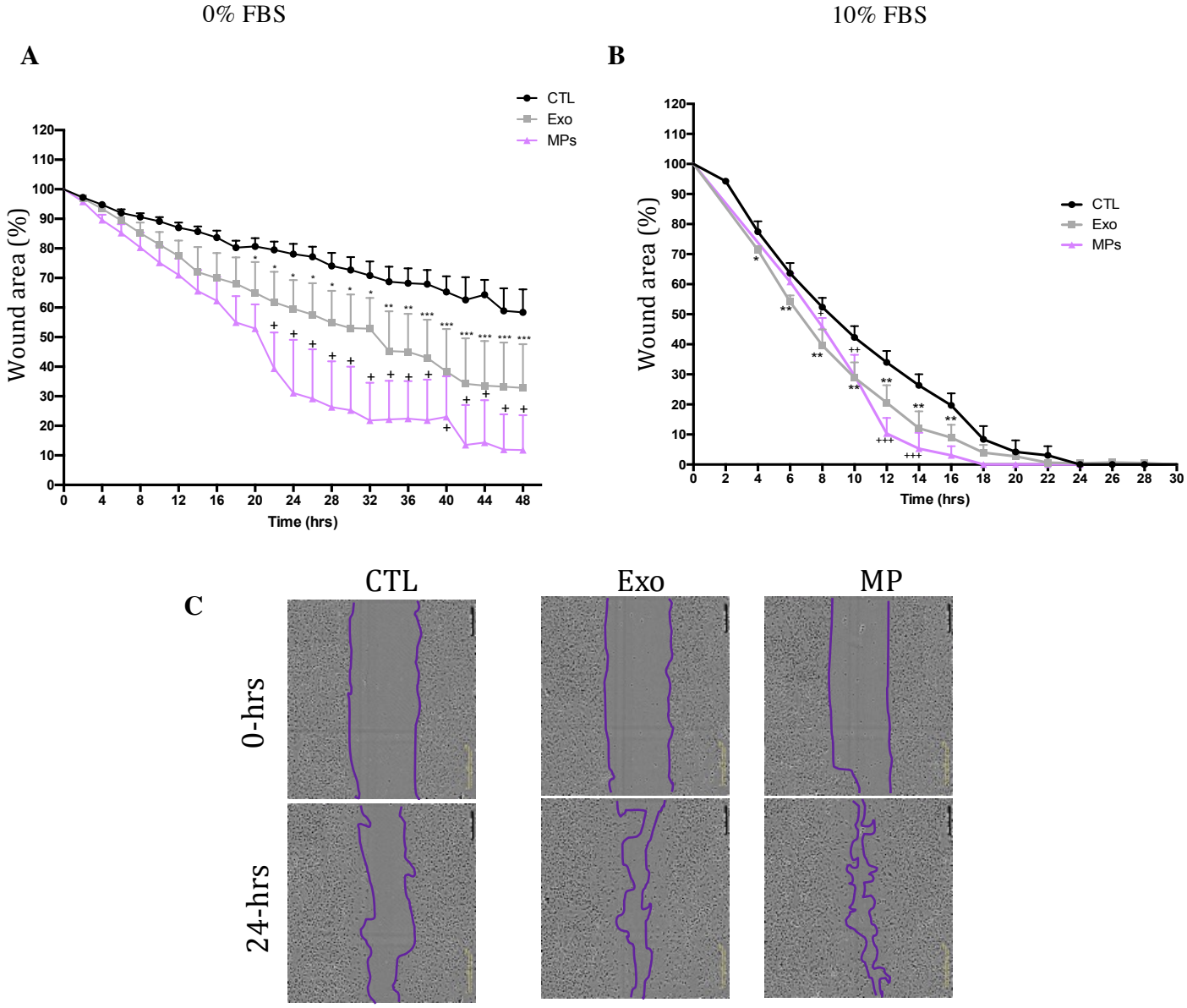

Figure 14. ECFC- derived exosomes and MPs stimulate REC migration in normoxia. Graphs show percent wound closure under **(A)** 0% FBS, * $p < 0.05$, ** $p < 0.01$, *** $p < 0.001$, + $p < 0.05$ vs. control (CTL). **(B)** 10% FBS, * $p < 0.05$, ** $p < 0.01$, *** $p < 0.001$, + $p < 0.05$, ++ $p < 0.01$, +++ $p < 0.001$ vs control (CTL) Values are means ± SEM, N= 4 for MPs and N=5 for exosomes. **(C)** Representative photomicrograph of the wound edge (the edges were drawn using powerpoint) in the scratch assay at 0 and 24h in 0% FBS. CTL, control; Exo, exosome (50 µg/mL); MPs, microparticles (50 µg/mL). Magnification 100x.

3. 4. 2. ECFC-derived exosomes and MPs promote REC migration in hypoxic conditions with serum starvation

We investigated the role of ECFC-derived exosomes and MPs on REC migration in hypoxic conditions. RECs were subjected to hypoxia for 24 hrs, and after scratch, cells were treated with 50 μg/ml of either exosomes or MPs at the time of reoxygenation.

Under serum starvation, ECFC-derived exosomes caused a dramatic increase in cellular migration by 12 hours after initiating wound scratch, with the wound closing in less than 48 hours. (**Fig. 15A, and C, *P < 0.05, ** P<0.01, *** P<0.001 vs control (CTL), n=5**). MPs modestly accelerated REC migration, with statistical significance being evident at the 47 and 48 hour mark (**+ p < 0.05 vs. control (CTL)) n=5 (Fig. 15A**). In contrast, in the presence of FBS, ECFC-derived exosomes and MPs exerted no significant effect on REC migration (**Fig. 15B**).

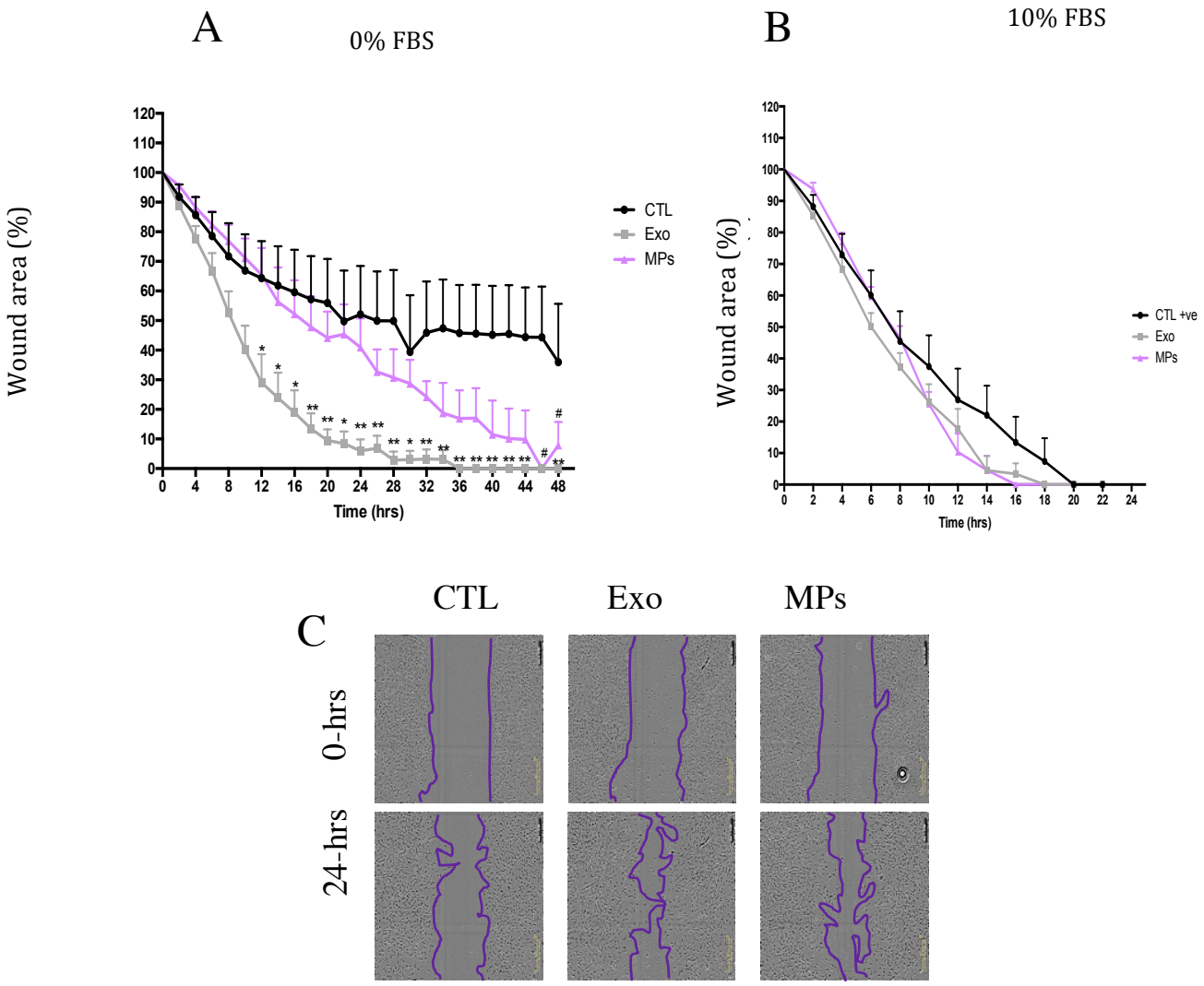

Figure 15. ECFC-derived extracellular vesicles promote REC migration in hypoxia. Graphs illustrate the percentage of wound closure under **(A)** 0% FBS, *P < 0.05, ** P<0.01, *** P<0.001 vs control (CTL), or **(B)** 10% FBS, n=5. **(C)** Representative photomicrograph of the wound edge in the scratch assay at 0 and 24h in 0% FBS. CTL, control; Exo, exosome (50 µg/mL), MPs, microparticles. Magnification 100x.

3. 4. 3. REC transfection with pre-MiR-486-5p increases the level of mature miR-486-5p

Prior to exploring the effect of miR-486-5p overexpression on REC migration, we evaluated the transfection quality using RT-PCR. Untransfected RECs showed very low levels of mature miR-486-5p. In contrast, the transfected group (pre-miR-486-5p, important for microRNA maturation) had a dramatic increase in the level of mature miR-486-5p levels after transfection **(Fig. 16).**

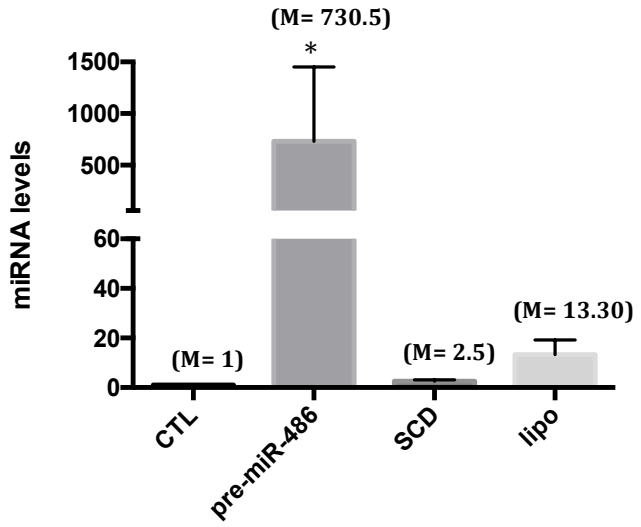

Figure 16. Transfection with pre-miR-486-5p increases the levels of mature miR-486-5p in RECs. RECs were transfected in 96-well plates using Lipofectamine. After 24-hrs, mature miR-486-5p was evaluated using real time polymerase chain reaction (qPCR). **CTL**; control (untransfected cells), **pre-miR-486-5p**; RECs transfected with pre-miR-486-5p, **SCD**; cells transfected with scrambled RNA, **lipo**; cells treated with Lipofectamine only, and **M**; mean (n=4). * $P < 0.05$ vs. CTL.

Further experiments were planned to determine the role of ECFC-derived exosomes and miR-486-5p on REC migration. However, at this point the cultured RECs did not display an ability to migrate after wound scratching, even under control conditions (without exosomes). Accordingly, we re-examined the RECs by staining them with CD31, to determine if they retained endothelial cell properties. We studied a different REC line purchased from the same company to compare with the original REC line. The original cells showed a slightly lower degree of CD31 expression compared to the newly purchased RECs, which could suggest that at some point the REC biology changed, and this is may be why cells did not respond to scratching (**Fig. 17**). The control cells (CTLs) (stained only with secondary antibody did not demonstrate expression of CD31. In addition, we found that the new batch of RECs exerted the same abnormal response as the old batch of RECs in the wound-healing assay. Therefore, because of the change in RECs properties, we decided to continue with HUVECs for the remainder of the project.

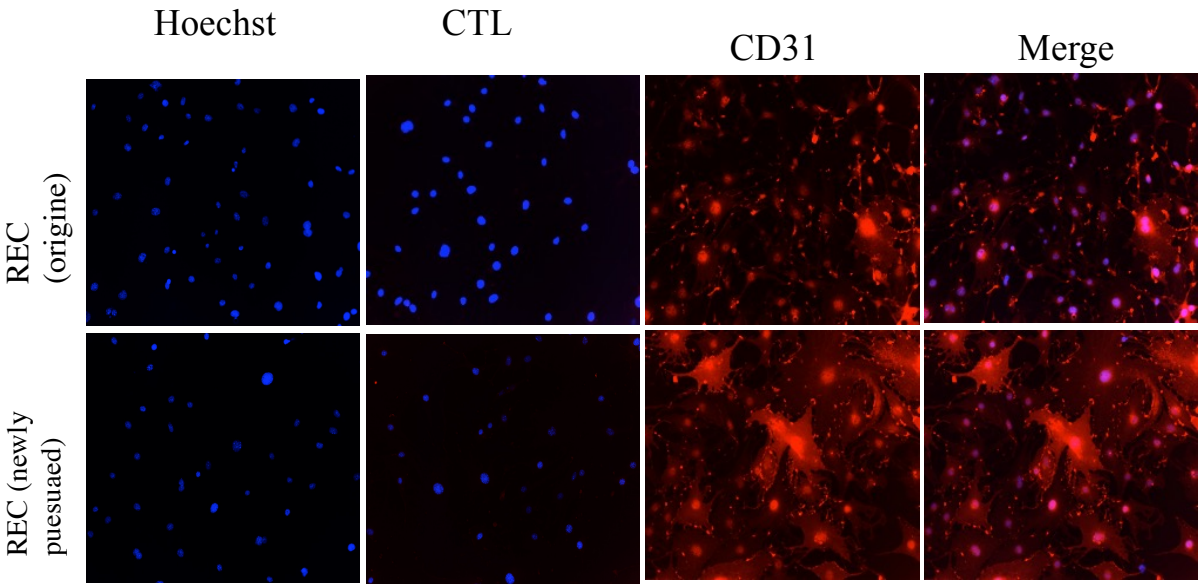

Figure 17. Original batch RECs express less CD31. RECs (original batch and newly purchased) were cultured in 6-well plates and stained with CD31 (red) antibodies. CTL; stained with secondary Ab only. Images shown are representative photomicrographs (N= 3), magnification 200X.

3. 4. 4. ECFC-derived exosomes accelerate wound healing in HUVECs under normoxic conditions

We conducted the wound-healing assay using HUVECs to explore the impact of ECFC-derived exosomes on cell migration in normoxic conditions. The experimental conditions were divided into four groups, with HUVECs being incubated in: i) 10% FBS as a positive control for maximum cell growth, ii) no FBS as a negative control for minimum cell growth, iii) 2% FBS as a control for comparison to the exosomes treatment group, and iv) 2% FBS plus treatment with 50 μg/ml ECFC-derived exosomes after wound scratch. Exosomes significantly increased cell migration 10 hrs after initiating the wound scratch assay, and closed the wound after roughly 18 hours (*$P < 0.05$, ** $P<0.01$, *** $P<0.001$ vs CTL (2% FBS), n=4. **(Fig.18)**.

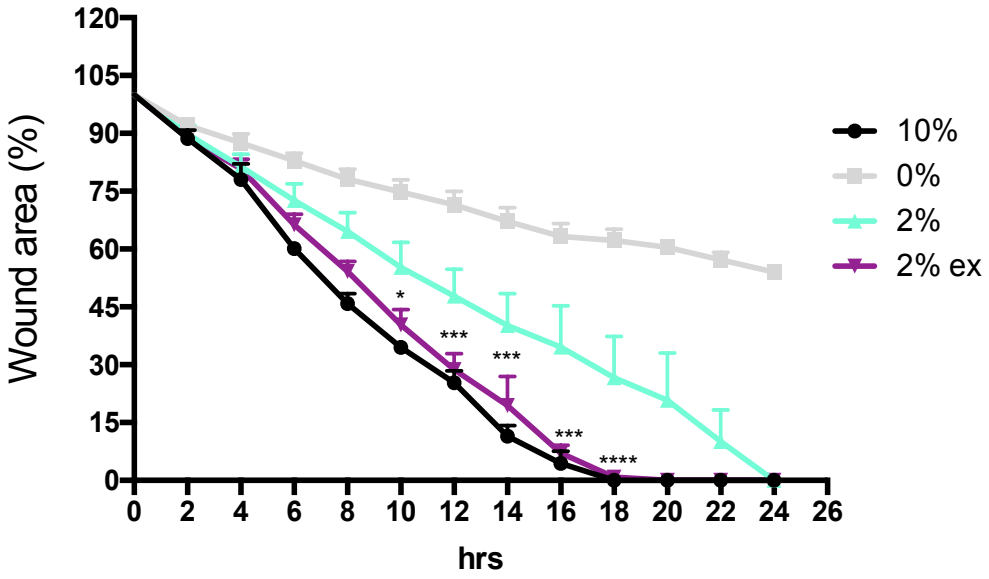

Figure 18. ECFC-derived exosomes accelerate HUVECs migration. Under normoxia conditions, HUVECs were scratched and treated with 50 µg/ml of ECFC-derived exosomes, and the effects of exosomes were observed over 24-hrs using IncuCyte imaging software. **10%;** HUVECs in 10% FBS, **0%;** HUVECs in free-FBS media, **2%;** HUVECs in 2% FBS, **2% ex;** HUVECs in 2% FBS then treated with 50 µg/ml of exosomes. *P < 0.05, ** P<0.01, *** P< 0.001 vs CTL (2% FBS), n=4.

3. 4. 5. Transfection of HUVEC with pre-MiRNA-486-5p increases the level of mature miRNA-486-5p

Because the RECs failed to migrate normally in response to scratch testing, we studied the role of miR-486-5p on migration in cultured HUVECs. We first transfected HUVECs with pre-miR-486-5p for 24 hrs at 37 ºC, and then we performed RT-PCR. Untransfected HUVECs showed very low levels of mature miR-486-5p, while the transfected group (pre-miR-486-5p) demonstrated a dramatic increase in miR-486-5-p levels (**Fig. 19, * p < 0.05 vs control (CTL), N= 3**).

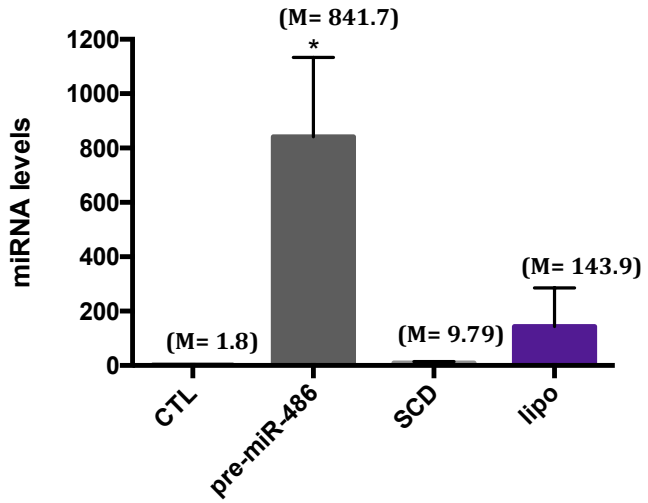

Figure 19. Transfection with pre-miR-486-5p increases the levels of mature miR-486-5p in HUVECs. HUVECs were transfected in 96-well plates using Lipofectamine. After 24-hrs, mature miR-486-5p was evaluated using real time polymerase chain reaction (qPCR). **CTL**; control (untransfected cells), **pre-miR-486-5p**; cells transfected with pre-miR-486-5p, **SCD**; cells transfected with scrambled RNA, **lipo**; cells treated with Lipofectamine only, and **M**; mean; (n=3). * $P < 0.05$ vs. CTL.

3. 4. 6. Transfection of HUVECs with pre-miR-486-5p accelerates HUVECs migration

After observing the remarkable effect of ECFC-derived exosomes on accelerating HUVEC migration under normoxic conditions, we further explored the role of miR-486-5-p, which is highly enriched in exosomes, on HUVEC migration.

We transfected HUVECs with pre-miR-486-5-p for 24 hours to over-express mature miR-486-5-p. HUVECs were incubated in three different conditions: i) 1% FBS as a control for minimum cell growth as/compared to transfected group, ii) 1% FBS plus transfection with pre-miR-486-5p, and iii)1% FBS plus treatment with 50 μg/ml of ECFC-derived exosomes after scratch (positive control). The results revealed that the HUVECs slowly migrated during the early hrs after scratch (between 2 hrs to 18 hrs) until the 20 hrs mark. After this time point, the transfected cells significantly increased their rate of migration, compared to untreated control cells (* $P<0.05$ vs CTL (HUVEC), n=3. **(Fig. 20)**). Furthermore, as expected ECFC-derived exosomes treatment caused a significant increase in cell migration (Fig. 19, + $p < 0.05$, ++ $p < 0.01$, +++ $p < 0.001$ vs control (CTL), n=3).

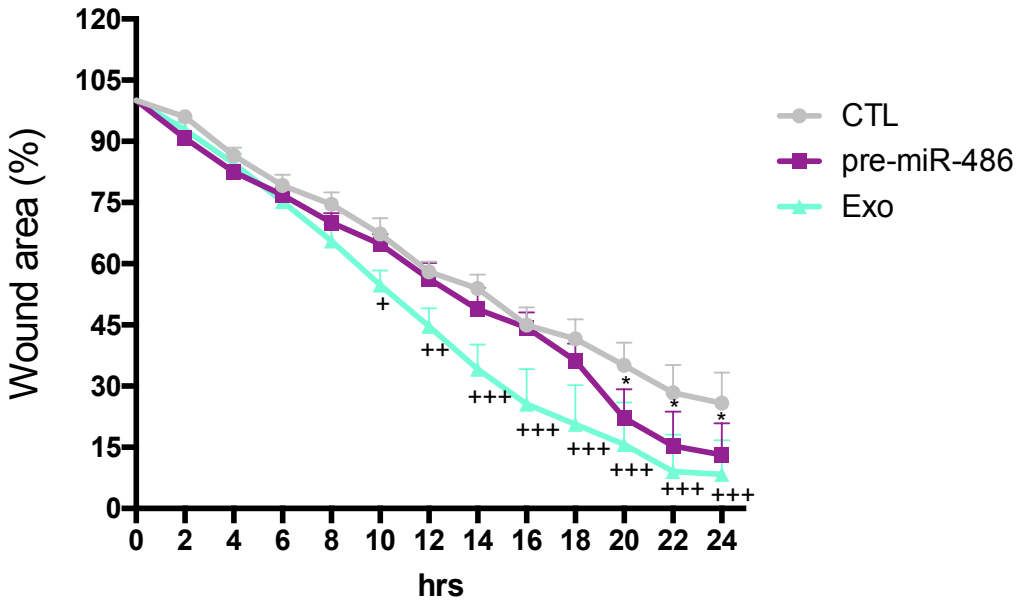

Figure 20. miR-486-5p stimulates HUVEC migration under normoxia. HUVECs were transfected with pre-miR-486-5p for 24-hrs, and then scratched using wound maker. Migration was observed over 24-hrs using IncuCyte imaging software. **CTL;** HUVECs in 1% FBS, **pre-miR-486;** HUVECs in 1% FBS and transfected with pre-miR-486-5p, **Exo;** HUVECs in 1% FBS and treated with 50 ug/ml of exosomes. * P< 0.01, + p < 0.05, ++ p < 0.01, +++ p < 0.001 vs control(CTL), n=3.

Chapter 4: Discussion

The purpose of this study was to assess the role ECFC-derived exosomes and MPs on endothelial cell behavior in hypoxia/reoxygenation (H/R) *in vitro*, to examine the possible pathway for exosome internalization into RECs/HUVECs, and to evaluate the effect of exosomes and miR-486-5p on endothelial cell migration. Our hypothesis involved three points: we hypothesized that ECFC-derived exosomes would enhance endothelial cell proliferation, and cell migration under normoxia and hypoxia conditions, but ECFC-derived MPs would attenuate endothelial cell proliferation and migration after H/R. We hypothesized that ECFC-derived exosomes would enter endothelial cells via macropinocytosis. Finally, we hypothesized that miR-486-5-p would exert similar effects on endothelial cell behavior compared to ECFC-derived exosomes.

The principal findings from this project are that ECFC-derived exosomes and MPs enhance cellular proliferation and migration in normoxia, in the absence of serum. In hypoxia, we observed that REC proliferation improved after exosome and MPs treatments. Moreover, ECFC-derived exosomes and MPs induced REC migration after hypoxic insult. ECFC-derived exosomes internalized into REC/HUVEC cytoplasm; however, it is not yet clear the exact pathway for uptake into RECs, but we

found exosomes enter into HUVECs via macropinocytosis. In addition, our data suggest that ECFC-derived exosomes stimulate HUVECs migration via miR-486-5p in normoxia. In conclusion, ECFC-derived exosomes protect endothelial cells from hypoxia by enhancing cellular proliferation rate. We propose that miR-486-5p may play a role in targeting RNAs that are involved in stimulating endothelial cell migration.

Endothelial cells were characterized by the presence of the endothelial-specific surface markers CD31 (Burger et al., 2015) and CD144 (VE-cadherin) (Kim et al., 2005). In our study, these markers were evaluated in REC and HUVEC cell lines by staining them with CD31 and CD144 antibodies. Our results were consistent with previous reports (Burger et al., 2015; Kim et al., 2005) (**Fig. 2**), indicating that RECs and HUVECs demonstrate the endothelial cell phenotype by expressing specific endothelial cell surface markers.

Several methods have been established to assess the purity of extracellular vesicles (EVs), either by evaluating vesicle surface markers (Burger et al., 2015; Li et al., 2018; Salomon et al., 2013; Viñas et al., 2016), the shape of the particles (exosomes have a caped shape) using a transmission electronic microscope (Li et al., 2018; Salomon et al., 2013), or

size distribution of the vesicles (exosomes (40 nm - 100 nm), MPs (100 nm - 1000 nm)) (Burger et al., 2015; Li et al., 2018; Viñas et al., 2016). Several surface antigens have been identified as exosome-specific markers, such as TSG101 (Burger et al., 2015), CD63, and CD9 (Li et al., 2018). In this particular study, we evaluated the expression of TSG101 in exosomes and MPs. We found that exosomes isolated from ECFCs expressed TSG101 while MPs did not, which is consistent with previous findings (**Fig. 3A**) (Burger et al., 2015; Viñas et al., 2016).

Nanoparticle tracking is another method to evaluate the purity of exosomes and MPs (Viñas et al., 2016), and size distribution of exosomes and MPs. In this study we determined that the purity and size distribution of exosomes and MPs were similar to findings from a previous study (Viñas et al., 2016). For exosomes, 81% were within the size range of 40-100 nm in diameter. For MPs, 78.6% were within the size range of 100 to 1000 nm (**Fig. 3B**). In conclusion, these data confirmed that the methodology we used to isolate exosomes and MPs from ECFC conditioned media, which was ultracentrifugation, isolated exosomes and MPs with a purity of over 75%.

In our previous study, we demonstrated that injecting human cord blood-derived ECFCs into mice with AKI attenuates renal endothelial cell

proliferation (Burger et al., 2015). However, other studies have indicated that MSCs/EPCs promote endothelial regeneration via paracrine actions (Biancone et al., 2012; Li et al., 2016). In addition, exosomes derived from MSCs (Gangadaran et al., 2017) and EPCs (Li et al., 2016) in a different ischemia model were found to stimulate endothelial cell proliferation. Therefore, in this study, RECs were chosen as a representative cell line model to study hypoxia/reoxygenation and to mimic the *in vivo* study in our previous report (Burger et al., 2015). Gangadaran et al. observed that MSC-derived microvesicles induce Mouse endothelial SVEC4-10EHR1 cell proliferation under serum starvation (Gangadaran et al., 2017). Similarly, we found that ECFC-derived exosomes increase REC proliferation under serum starvation in normoxia (**Fig. 4A**). ECFC-derived MPs were used as vesicles of comparison, and revealed a similar pattern to that observed with ECFC-derived exosomes (**Fig. 4A**). Despite these findings, exosomes and MPs did not promote proliferation in the presence of serum (**Fig. 4B**). Taken together, and consistent with previous findings (Gangadaran et al., 2017), exosomes and MPs were able to protect RECs from injury, which is normally caused by the absence of serum.

In contrast, in the presence of serum, the cells may have reached a state of maximal proliferative response, and that may be why exosomes and

MPs did not show a further enhancement in cell proliferation (**Fig. 4B**). When we treated RECs with a lower concentration of exosomes (7.5 μg/ml), in normoxia, the RECs did not proliferate, either with/or without FBS. One possible explanation for this is that the exosome concentration may have been too low to have any effect on the cells, but the FBS in the experiment (CTL; 0%, and CTL; 10% FBS) did not affect RECs, and did not increase the degree of proliferation, so we cannot make a definite conclusion with regards to REC proliferation (**Fig. 5**).

Exosomes released from human-induced pluripotent stem cell (iPSC)-derived MSCs increased endothelial cell proliferation in a limb ischemia model (Hu et al., 2015). Others have reported that placental MSC (pMSCc)-derived exosomes stimulate human placenta microvascular endothelial cell (hPMEC) proliferation under hypoxic conditions (Salomon et al., 2013). In our study, ECFC-derived exosomes tended to increase REC proliferation in H/R conditions. Although these findings were not statistically significant, ECFC-derived exosomes displayed a similar trend to those found in other studies (Salomon et al., 2013) (**Fig. 6A**). On the other hand, serum protects RECs from apoptosis, and ECFC-derived exosomes did not induce further proliferation (**Fig. 6B**). In addition, Kim et al. indicated that platelet-derived microparticles protect endothelial cells from apoptosis (Kim et al., 2004).

Furthermore, Brill at al. found that platelet-derived MPs induce endothelial proliferation in ischemia (Brill et al., 2005). In our study, ECFC-derived MPs displayed a similar pattern of stimulating REC proliferation in serum-free conditions (**Fig. 6A**). However, our findings suggest that the presence of serum increased REC proliferation, with no further effect of MPs. It is possible that REC proliferation was maximized, which could explain why ECFC-derived MPs did not induce further proliferation (**Fig. 6B**).

As noted previously our *in vivo* studies revealed that renal endothelial cell proliferation was attenuated after injecting ECFCs into mice with renal ischemic injury (Burger et al., 2015). In the current studies, ECFC-conditioned media (CM) (to mimic the *in vivo* study), did not affect cell proliferation (**Fig. 6B**). Since exosomes and MPs increased REC proliferation individually, ECFCs may release inhibitory factors that attenuate renal endothelial cell proliferation, as suggested in the previous *in vivo* model (Burger et al., 2015).

Accumulating evidence illustrates that EVs derived from pluripotent stem cells (Hu et al., 2015) and endothelial progenitor cells (EPCs) (Deregibus et al., 2007) stimulate HUVEC proliferation. In this study, however, we found that ECFC-derived exosomes and MPs had no effect on HUVEC

proliferation under normoxia and hypoxia (**Fig. 7**). Indeed, the concentration of ECFC-derived exosomes (7.5 μg/ml) may have been too low to exert any effects on cellular proliferation in normoxia (**Fig. 8A, and B**). In addition, when cells were treated with ECFC-conditioned media, there was no significant effect on cell proliferation in hypoxia (**Fig. 9**). When HUVECs were treated with exosomes and MPs separately, each condition induced a mild increase in proliferation compared to cells treated with ECFC-conditioned medium. These findings suggest that there may be inhibitory factors that attenuate the proliferative effects induced by exosomes and MPs. In conclusion, our data suggest that the effect of ECFC-derived exosomes and MPs on renal endothelial proliferation is dependent on the specific cell type.

Recent studies indicate that exosomes may act to carry information from cell to cell. This information transfer process is carried out by attaching or internalizing into the recipient cell (Tian et al., 2014). Furthermore, several physiological and pathological mechanisms, such as antigen presentation, are mediated via the paracrine action of exosomes (Cai et al., 2012; Tian et al., 2014). Exosome tracking was visualised by real-time fluorescence microscopy and single particle tracking. However, exosome particle

trafficking via endocytosis, as a particular pathway, has not been previously visualized (Tian et al., 2014).

There are number of pathways that mediate various forms of endocytosis, such as phagocytosis, macropinocytosis, and clathrin-mediated endocytosis (Tian et al., 2014). In this project, we examined exosomes entering the cell via macropinocytosis and clathrin-mediated endocytosis. We used EIPA and LY294002 to inhibit macropinocytosis, and CPZ to inhibit clathrin-mediated endocytosis. First, we examined REC morphology after EIPA treatment only. In normal conditions, endothelial cells are elongated, and held together by tight junctions (Aird, 2012; Huang et al., 2013). Our findings revealed a similar pattern of endothelial cell morphology (**Fig. 10**) compared to previous studies (Aird, 2012; Huang et al., 2013). After inhibiting macropinocytosis with EIPA in normoxic conditions, the number of internalizing particles in REC did not change (**Fig. 11A, and B**). This outcome was consistent with what Tian et al. reported, using the same concentration (10 μl) of EIPA (Tian et al., 2014). In a previous study, we reported that blocking macropicocytosis in HUVECs with 10 μM of EIPA in normoxia led to a dramatic decrease in the uptake of PKH26-labled exosomes (**Fig. 13B, and C**) (Viñas et al., 2016). When RECs were exposed to the same conditions, however, macropinocytosis was not

observed (Viñas et al., 2016). Feng et al. reported that exosomes isolated from erythroleukemia cells were internalized via phagocytosis, but not via macropinocytosis (Feng et al., 2010), which indicates that the uptake of exosomes may be dependent on the specific cell type (Tian et al., 2014). Tian et al. blocked macropinocytosis and clathrin-mediated endocytosis using LY294002 and CPZ respectively, and found that exosome uptake was significantly decreased in the presence of CPZ (10 μl), and LY294002 (10, 20, 50μl) (Tian et al., 2014). After performing a pooled analysis for each treatment (LY294002, and CPZ), we observed a similar pattern(significant inhibition for each agent when analysed as pooled concentrations), but our data were not statically significant at individual concentrations (**Fig. 12**). Overall, ECFC-derived exosomes internalize into HUVECs via macropinocytosis, while exosomes are internalized via macropinocytosis and clathrin-mediated endocytosis. In RECs, however, further experiments are needed to confirm the mechanisms of exosome internalization.

It has been reported that endothelial cell migration is an important physiological mechanism (Michaelis, 2014). This is especially important during vascular damage, because endothelial cell migration can restore vessel integrity (Michaelis, 2014). While the role of exosomes on endothelial cell migration has been evaluated in several studies, the role of

MPs on endothelial cell migration is less understood. The Zhao group incubated human umbilical vein endothelial cells (EA.hy926) with exosomes, isolated from human umbilical-cord mesenchymal stem cells (UC-MSCs), in an acute myocardial ischemia injury model. They reported a significant increase in cellular migration (Mao et al., 2017). Another group found that human umbilical-cord mesenchymal stem cell-derived exosomes promoted EA.hy926 endothelial cell migration after 12 and 24 hours of incubation, in a dose dependent-manner (Zhang et al., 2015). In this project, we demonstrated that ECFC-derived exosomes accelerated REC migration in a serum-free environment, throughout the incubation duration (48 hours) in normoxia. As a comparison, the impact of ECFC-derived MPs on REC migration was greater than that exerted by the exosomes (**Fig. 14A, and C**). We found similar effects for both exosomes and MPs in the presence of serum (**Fig. 14B**). In addition, under serum-starved conditions in hypoxia we showed that exosomes dramatically increase cellular migration (**Fig. 15A**), but we did not find any changes in the presence of serum (**Fig. 15B**). Overall, these findings suggest that ECFC-derived exosomes and MPs protect RECs after hypoxia-induced ischemia, which is consistent with other findings.

In a previous study, we reported that ECFC-derived exosomes are highly enriched with miR-486-5p. In addition, we indicated that miR-486-5p plays a role in preventing ischemia-induced apoptosis by inhibiting PTEN and thus increasing the phosphorylation of Akt (Viñas et al., 2016). After we witnessed the dramatic effect of ECFC-derived exosomes on REC migration, particularly in hypoxia under serum starved conditions, it raised the question of whether miR-486-5p was involved. Thus, to examine this hypothesis in depth, we transfected RECs with pre-miR- 486-5p, which is important for miR biogenesis, to increase the production of miR-486-5p. We observed that RECs do not normally express miR-486-5p, as do ECFCs (**Fig. 16**). However, because of unexpected cells outcome we decided to continue with HUVECs.

We showed that HUVECs displayed similar migratory responses to what was found in previous reports, and also similar to what we found initially in RECs in normoxia under serum-starved condition (2% FBS) (Zhang et al., 2015) (**Fig. 18**). Collino et al. found that a global down regulation in miR expression in MSCs, induced by Dorsha knockdown, inhibited the regenerative ability of MSC- derived EVs, and abrogated renal recovery after ischemic AKI (Collino et al., 2015). We performed a wound-healing assay on HUVECs transfected with pre-miR-486-5p, and another group of

HUVECs treated with exosomes as a control to compare with the transfected group. Interestingly, the transfected group showed a significant stimulation of HUVEC migration at 20, 22 and 24 hours (**Fig. 20**), which suggests that cells were in the process of generating mature miR-486-5p for the first 19 hours. HUVECs then miR- 486-5p, which could be the underlying cause of the increase in their migration.

Dellet et al. reported that ECFC-derived EVs increase human retinal microvascular endothelial cell (hRMEC) migration in ischemic retinopathy, which was reflected by microarray assay (Dellett et al., 2017). Their microarray findings revealed a significant increase in the expression of genes that are related to angiogenesis (proliferation and migration) (Dellett et al., 2017). In addition, they reported that ECFC-EVs contained a high concentration of various miRs, which mostly target genes involved in angiogenesis (Dellett et al., 2017). These findings support our data, and indicate the roles of ECFC-derived EVs (exosomes and MPs), and their miR content in protecting endothelial cells from ischemia, as well as inducing endothelial cell recovery after ischemia.

Taken together, the findings from this study suggest a possible signalling pathway for ECFC-derived exosomes and miR-486-5p in inducing endothelial cell proliferation and migration, which is illustrated in **Fig. 21**.

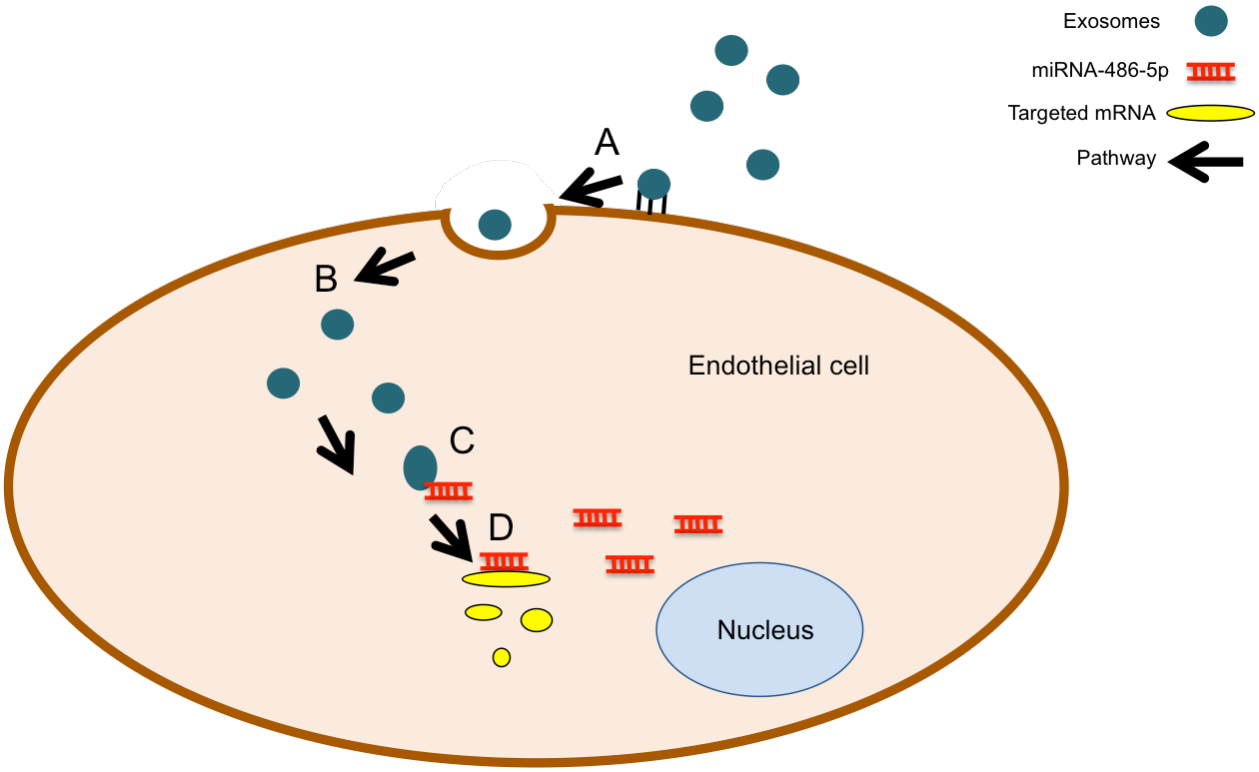

Fig. 21. The molecular pathway for ECFC-derived exosomes and its miR-486-5p in endothelial cells. A) Exosomes attached to the cell surface molecules allowing for exosomes internalization. B) Exosomes enter the cell via endocytosis. C) Exosomes infuse their cargo, including miR-486-5p. D) miRNA-486-5p bind to the target mRNA and block the target mRNA function.

Chapter 5: Future direction

In order to increase the strength of our data and gain a better understanding of the role of ECFC-derived exosomes and miR-486-5p, suggested future assessments would be to:

1) Determine the effect of ECFC-derived exosomes on HUVECs in hypoxia.

2) Examine and assess the role of miR-486-5p overexpression on HUVEC migration in hypoxia.

3) Assess the effects of ECFC-derived exosomes with miR-486-5p knockdown, and compare the outcomes with miR-486-5p overexpression in normoxia and hypoxia.

4) Examine, in depth, the effects of ECFC-derived exosomes and miR-486-5p on the signalling pathways for endothelial cell proliferation (e.g Bcl2, Wnt) and migration (e.g Cdc42, Rac).

5) Assess the roles of ECFC-exosomes and miR-486-5p in *in vivo* studies, and compare these findings with

in vitro findings.

These proposed experiments will improve our understanding in depth.

References:

Aird, W.C. (2012). Endothelial Cell Heterogeneity. Cold Spring Harb. Perspect. Med. *2*.

Asahara, T., Murohara, T., Sullivan, A., Silver, M., van der Zee, R., Li, T., Witzenbichler, B., Schatteman, G., and Isner, J.M. (1997). Isolation of putative progenitor endothelial cells for angiogenesis. Science *275*, 964–967.

Au, P., Daheron, L.M., Duda, D.G., Cohen, K.S., Tyrrell, J.A., Lanning, R.M., Fukumura, D., Scadden, D.T., and Jain, R.K. (2008). Differential in vivo potential of endothelial progenitor cells from human umbilical cord blood and adult peripheral blood to form functional long-lasting vessels. Blood *111*, 1302–1305.

Bagshaw, S.M., Bellomo, R., Devarajan, P., Johnson, C., Karvellas, C.J., Kutsiogiannis, D.J., Mehta, R., Pannu, N., Romanovsky, A., Sheinfeld, G., et al. (2010). [Review article: Acute kidney injury in critical illness]. Can. J. Anaesth. J. Can. Anesth. *57*, 985–998.

van Balkom, B.W.M., Pisitkun, T., Verhaar, M.C., and Knepper, M.A. (2011). Exosomes and the kidney: prospects for diagnosis and therapy of renal diseases. Kidney Int. *80*, 1138–1145.

Baraniak, P.R., and McDevitt, T.C. (2010). Stem cell paracrine actions and tissue regeneration. Regen. Med. *5*, 121–143.

Basile, D.P., and Yoder, M.C. (2014). Renal endothelial dysfunction in acute kidney ischemia reperfusion injury. Cardiovasc. Hematol. Disord. Drug Targets. *14*, 3–14.

Berridge, M.J. (2014). Module 9: Cell Cycle and Proliferation. Cell Signal. Biol. *6*, csb0001009.

Bonventre, J.V., and Yang, L. (2011). Cellular pathophysiology of ischemic acute kidney injury. J. Clin. Invest. *121*, 4210–4221.

Brill, A., Dashevsky, O., Rivo, J., Gozal, Y., and Varon, D. (2005). Platelet-derived microparticles induce angiogenesis and stimulate post-ischemic revascularization. Cardiovasc. Res. *67*, 30–38.

Brodsky, S.V., Yamamoto, T., Tada, T., Kim, B., Chen, J., Kajiya, F., and Goligorsky, M.S. (2002). Endothelial dysfunction in ischemic acute renal failure: rescue by transplanted endothelial cells. Am. J. Physiol. Renal Physiol. *282*, F1140-1149.

Burger, D., Gutsol, A., Carter, A., Allan, D.S., Touyz, R.M., and Burns, K.D. (2012). Human cord blood CD133+ cells exacerbate ischemic acute kidney injury in mice. Nephrol. Dial. Transplant. Off. Publ. Eur. Dial. Transpl. Assoc. - Eur. Ren. Assoc. 27, 3781–3789.

Burger, D., Schock, S., Thompson, C.S., Montezano, A.C., Hakim, A.M., and Touyz, R.M. (2013). Microparticles: biomarkers and beyond. Clin. Sci. Lond. Engl. 1979 *124*, 423–441.

Burger, D., Viñas, J.L., Akbari, S., Dehak, H., Knoll, W., Gutsol, A., Carter, A., Touyz, R.M., Allan, D.S., and Burns, K.D. (2015). Human endothelial colony-forming cells protect against acute kidney injury: role of exosomes. Am. J. Pathol. *185*, 2309–2323.

Cai, Z., Zhang, W., Yang, F., Yu, L., Yu, Z., Pan, J., Wang, L., Cao, X., and Wang, J. (2012). Immunosuppressive exosomes from TGF-β1 gene-modified dendritic cells attenuate Th17-mediated inflammatory autoimmune disease by inducing regulatory T cells. Cell Res. *22*, 607–610.

Cantaluppi, V., Gatti, S., Medica, D., Figliolini, F., Bruno, S., Deregibus, M.C., Sordi, A., Biancone, L., Tetta, C., and Camussi, G. (2012). Microvesicles derived from endothelial progenitor cells protect the kidney from ischemia-reperfusion injury by microRNA-dependent reprogramming of resident renal cells. Kidney Int. *82*, 412–427.

Choi, H.Y., Moon, S.J., Ratliff, B.B., Ahn, S.H., Jung, A., Lee, M., Lee, S., Lim, B.J., Kim, B.S., Plotkin, M.D., et al. (2014). Microparticles from kidney-derived mesenchymal stem cells act as carriers of proangiogenic signals and contribute to recovery from acute kidney injury. PloS One *9*, e87853.

Collino, F., Bruno, S., Incarnato, D., Dettori, D., Neri, F., Provero, P., Pomatto, M., Oliviero, S., Tetta, C., Quesenberry, P.J., et al. (2015). AKI Recovery Induced by Mesenchymal Stromal Cell-Derived Extracellular Vesicles Carrying MicroRNAs. J. Am. Soc. Nephrol. JASN *26*, 2349–2360.

Colombo, M., Raposo, G., and Théry, C. (2014). Biogenesis, secretion, and intercellular interactions of exosomes and other extracellular vesicles. Annu. Rev. Cell Dev. Biol. *30*, 255–289.

Delenclos, M., Trendafilova, T., Mahesh, D., Baine, A.M., Moussaud, S., Yan, I.K., Patel, T., and McLean, P.J. (2017). Investigation of Endocytic Pathways for the Internalization of Exosome-Associated Oligomeric Alpha-Synuclein. Front. Neurosci. *11*.

Dellett, M., Brown, E.D., Guduric-Fuchs, J., O'Connor, A., Stitt, A.W., Medina, R.J., and Simpson, D.A. (2017). MicroRNA-containing extracellular vesicles released from endothelial colony-forming cells modulate angiogenesis during ischaemic retinopathy. J. Cell. Mol. Med. *21*, 3405–3419.

Deregibus, M.C., Cantaluppi, V., Calogero, R., Lo Iacono, M., Tetta, C., Biancone, L., Bruno, S., Bussolati, B., and Camussi, G. (2007). Endothelial progenitor cell derived microvesicles activate an angiogenic program in endothelial cells by a horizontal transfer of mRNA. Blood *110*, 2440–2448.

Farooqi, A.A., Desai, N.N., Qureshi, M.Z., Librelotto, D.R.N., Gasparri, M.L., Bishayee, A., Nabavi, S.M., Curti, V., and Daglia, M. (2017). Exosome biogenesis, bioactivities and functions as new delivery systems of natural compounds. Biotechnol. Adv.

Feng, D., Zhao, W.-L., Ye, Y.-Y., Bai, X.-C., Liu, R.-Q., Chang, L.-F., Zhou, Q., and Sui, S.-F. (2010). Cellular internalization of exosomes occurs through phagocytosis. Traffic Cph. Den. *11*, 675–687.

Fukuhara, S., Zhang, J., Yuge, S., Ando, K., Wakayama, Y., Sakaue-Sawano, A., Miyawaki, A., and Mochizuki, N. (2014). Visualizing the cell-cycle progression of endothelial cells in zebrafish. Dev. Biol. *393*, 10–23.

Grange, C., Moggio, A., Tapparo, M., Porta, S., Camussi, G., and Bussolati, B. (2014a). Protective effect and localization by optical imaging of human renal CD133+ progenitor cells in an acute kidney injury model. Physiol. Rep. *2*, e12009.

Grange, C., Tapparo, M., Bruno, S., Chatterjee, D., Quesenberry, P.J., Tetta, C., and Camussi, G. (2014b). Biodistribution of mesenchymal stem cell-derived extracellular vesicles in a model of acute kidney injury monitored by optical imaging. Int. J. Mol. Med. *33*, 1055–1063.

Gulyaeva, L.F., and Kushlinskiy, N.E. (2016). Regulatory mechanisms of microRNA expression. J. Transl. Med. *14*, 143.

György, B., Szabó, T.G., Pásztói, M., Pál, Z., Misják, P., Aradi, B., László, V., Pállinger, E., Pap, E., Kittel, A., et al. (2011). Membrane vesicles, current state-of-the-art: emerging role of extracellular vesicles. Cell. Mol. Life Sci. CMLS *68*, 2667–2688.

Huang, N.F., Okogbaa, J., Lee, J.C., Jha, A., Zaitseva, T.S., Paukshto, M.V., Sun, J.S., Punjya, N., Fuller, G.G., and Cooke, J.P. (2013). The modulation of endothelial cell morphology, function, and survival using anisotropic nanofibrillar collagen scaffolds. Biomaterials *34*, 4038–4047.

Hu, G., Li, Q., Niu, X., Hu, B., Liu, J., Zhou, S., Guo, S., Lang, H., Zhang, C., Wang, Y., et al. (2015). Exosomes secreted by human-induced pluripotent stem cell-derived mesenchymal stem cells attenuate limb ischemia by promoting angiogenesis in mice. Stem Cell Res. Ther. *6*, 10.

Hristov, M., Erl, W., and Weber, P.C. (2003). Endothelial progenitor cells: mobilization, differentiation, and homing. Arterioscler. Thromb. Vasc. Biol. *23*, 1185–1189.

Hu, G., Li, Q., Niu, X., Hu, B., Liu, J., Zhou, S., Guo, S., Lang, H., Zhang, C., Wang, Y., et al. (2015). Exosomes secreted by human-induced pluripotent stem cell-derived mesenchymal stem cells attenuate limb ischemia by promoting angiogenesis in mice. Stem Cell Res. Ther. *6*, 10.

Jung, H.J., and Suh, Y. (2014). Circulating miRNAs in ageing and ageing-related diseases. J. Genet. Genomics Yi Chuan Xue Bao *41*, 465–472.

Kim, H.K., Song, K.S., Chung, J.-H., Lee, K.R., and Lee, S.-N. (2004). Platelet microparticles induce angiogenesis in vitro. Br. J. Haematol. *124*, 376–384.

Lertkiatmongkol, P., Liao, D., Mei, H., Hu, Y., and Newman, P.J. (2016). Endothelial functions of platelet/endothelial cell adhesion molecule-1 (CD31). Curr. Opin. Hematol. *23*, 253–259.

Liang, C.-J., Shen, W.-C., Chang, F.-B., Wu, V.-C., Wang, S.-H., Young, G.-H., Tsai, J.-S., Tseng, Y.-C., Peng, Y.-S., and Chen, Y.-L. (2015). Endothelial Progenitor Cells Derived From Wharton's Jelly of Human Umbilical Cord Attenuate Ischemic Acute Kidney Injury by Increasing

Vascularization and Decreasing Apoptosis, Inflammation, and Fibrosis. Cell Transplant. *24*, 1363–1377.

Liu, X., Li, Q., Niu, X., Hu, B., Chen, S., Song, W., Ding, J., Zhang, C., and Wang, Y. (2017). Exosomes Secreted from Human-Induced Pluripotent Stem Cell-Derived Mesenchymal Stem Cells Prevent Osteonecrosis of the Femoral Head by Promoting Angiogenesis. Int. J. Biol. Sci. *13*, 232–244.

Makris, K., and Spanou, L. (2016). Acute Kidney Injury: Definition, Pathophysiology and Clinical Phenotypes. Clin. Biochem. Rev. *37*, 85–98.

Mao, F., Wu, Y., Tang, X., Kang, J., Zhang, B., Yan, Y., Qian, H., Zhang, X., and Xu, W. (2017). Exosomes Derived from Human Umbilical Cord Mesenchymal Stem Cells Relieve Inflammatory Bowel Disease in Mice. BioMed Res. Int. *2017*.

Michaelis, U.R. (2014). Mechanisms of endothelial cell migration. Cell. Mol. Life Sci. *71*, 4131–4148.

Moubarik, C., Guillet, B., Youssef, B., Codaccioni, J.-L., Piercecchi, M.-D., Sabatier, F., Lionel, P., Dou, L., Foucault-Bertaud, A., Velly, L., et al. (2011). Transplanted late outgrowth endothelial progenitor cells as cell therapy product for stroke. Stem Cell Rev. *7*, 208–220.

Napoli, C., Hayashi, T., Cacciatore, F., Casamassimi, A., Casini, C., Al-Omran, M., and Ignarro, L.J. (2011). Endothelial progenitor cells as therapeutic agents in the microcirculation: an update. Atherosclerosis *215*, 9–22.

Patschan, D., Patschan, S., and Müller, G.A. (2011). Endothelial progenitor cells in acute ischemic kidney injury: strategies for increasing the cells' renoprotective competence. Int. J. Nephrol. *2011*, 828369.

Pei, D., Xu, J., Zhuang, Q., Tse, H.-F., and Esteban, M.A. (2010). Induced pluripotent stem cell technology in regenerative medicine and biology. Adv. Biochem. Eng. Biotechnol. *123*, 127–141.

Salomon, C., Ryan, J., Sobrevia, L., Kobayashi, M., Ashman, K., Mitchell, M., and Rice, G.E. (2013). Exosomal signaling during hypoxia mediates microvascular endothelial cell migration and vasculogenesis. PloS One *8*, e68451.

Sharfuddin, A.A., and Molitoris, B.A. (2011). Pathophysiology of ischemic acute kidney injury. Nat. Rev. Nephrol. *7*, 189–200.

Sun, J., Li, Y., Granziani, G., Filion, L., Allan, D. (2013). E-Selectin Mediated Adhesion and Migration of Endothelial Colony Forming Cells Is Enhanced by SDF-1a/CXCR4. PloS One. 8, e60890.

Takahashi, Y., Nishikawa, M., Shinotsuka, H., Matsui, Y., Ohara, S., Imai, T., and Takakura, Y. (2013). Visualization and in vivo tracking of the exosomes of murine melanoma B16-BL6 cells in mice after intravenous injection. J. Biotechnol. *165*, 77–84.

Tian, T., Zhu, Y.-L., Zhou, Y.-Y., Liang, G.-F., Wang, Y.-Y., Hu, F.-H., and Xiao, Z.-D. (2014). Exosome uptake through clathrin-mediated endocytosis and macropinocytosis and mediating miR-21 delivery. J. Biol. Chem. *289*, 22258–22267.

Vestweber, D. (2008). VE-cadherin: the major endothelial adhesion molecule controlling cellular junctions and blood vessel formation. Arterioscler. Thromb. Vasc. Biol. *28*, 223–232.

Viñas, J.L., Burger, D., Zimpelmann, J., Haneef, R., Knoll, W., Campbell, P., Gutsol, A., Carter, A., Allan, D.S., and Burns, K.D. (2016). Transfer of microRNA-486-5p from human endothelial colony forming cell-derived exosomes reduces ischemic kidney injury. Kidney Int. *90*, 1238–1250.

Wang, S., Amato, K.R., Song, W., Youngblood, V., Lee, K., Boothby, M., Brantley-Sieders, D.M., and Chen, J. (2015). Regulation of endothelial cell proliferation and vascular assembly through distinct mTORC2 signaling pathways. Mol. Cell. Biol. *35*, 1299–1313.

Yamamoto, T., Tada, T., Brodsky, S.V., Tanaka, H., Noiri, E., Kajiya, F., and Goligorsky, M.S. (2002). Intravital videomicroscopy of peritubular capillaries in renal ischemia. Am. J. Physiol. Renal Physiol. *282*, F1150-1155.

Yoder, M.C. (2012). Human endothelial progenitor cells. Cold Spring Harb. Perspect. Med. *2*, a006692.

Zhang, B., Wu, X., Zhang, X., Sun, Y., Yan, Y., Shi, H., Zhu, Y., Wu, L., Pan, Z., Zhu, W., et al. (2015). Human umbilical cord mesenchymal stem cell exosomes enhance angiogenesis through the Wnt4/β-catenin pathway.

Stem Cells Transl. Med. *4*, 513–522.